Supporting Information

Insights into the different mechanistic stages of light-induced hydrogen evolution of a 5,5'-bisphenanthroline linked RuPt complex

Martin Lämmle,[a,] T. David Pilz,[a,b,] Roger Jan Kutta,[c] Marius Müßler,[a] Alexander K. Mengele,[a] Helmar Görls,[d] Frank W. Heinemann,[b] Sven Rau*[a]

[a]Institute of Inorganic Chemistry I, Ulm University, Albert-Einstein-Allee 11, 89081 Ulm, Germany. E-mail: sven.rau@uni-ulm.de

[b]Department Chemistry and Pharmacy, Chair of Inorganic and General Chemistry, Friedrich-Alexander-Universität Erlangen-Nürnberg, Egerlandstraße 1, 91058 Erlangen, Germany.

[c]Institute of Physical and Theoretical Chemistry, University Regensburg, Universitätsstraße 31, 93053 Regensburg, Germany.

[d]Institute of Inorganic and Analytical Chemistry, Friedrich-Schiller-University Jena, Lessingstraße 8 – 10, 07743 Jena, Germany.

Table of contents

1. Chemicals

5-Bromo-1,10-phenanthroline[1], $[(tbbpy)_2RuCl_2]$[2], $[(tbbpy)PtCl_2]$[3] and $[PtCl_2(DMSO)_2]$[4] were synthesized according to literature procedures. Oleum (65%), bromine, NaOH, 25w% aqueous ammonia, $NiCl_2 \times 6H_2O$, triphenylphosphine, potassium cyanide, acetonitrile, tetrabutylammonium iodide (TBAI), 4,4'-di-*tert*-butyl-2,2'-bipyridine (tbbpy) and triethylamine (TEA) were purchased from commercial suppliers and used without further purification. All solvents were distilled before usage. All ^{1}H-NMR signals were assigned using 2D-NMR techniques. For **phenphen**, the assignment was based on H,H-COSY in agreement to Nakano *et al*..[5]

The freeze-pump-thaw technique was used to remove high amounts of molecular oxygen (O_2) from the samples used in the time-resolved spectroscopic experiments. The O_2 concentration in MeCN is about 2.4 mM under ambient conditions[6] and could be reduced down to the µM range under the used conditions for the freeze-pump-thaw technique[7].

For synthesis as well as for catalysis, molecular oxygen (O_2) was removed by bubbling argon through the respective solvent/solution (at least 1 min/mL) and subsequent utilization of standard schlenk technique.

2. Instrumentation

Steady state and time-resolved UV/vis absorption and emission spectroscopy. The steady state photophysical characterization was performed in (non)-degassed MeCN (Carl Roth, spectroscopic grade) at room temperature. The UV/Vis absorption spectra were measured either with JASCO V-670 or a Perkin Elmer Lambda 9a spectrometer. The emission spectra were measured with a Horiba Jobin Yvon Fluorolog-3 steady-state fluorescence spectrometer. The emission decays were recorded with a Horiba Jobin Yvon Fluorolog-3 spectrometer using a PicoBright PB-375 pulsed diode laser (λ_{exc} = 375 nm, pulse width 100 ps) as excitation source and a cooled photomultiplier attached to a FAST ComTec multichannel scalar PCI card with a time resolution of 250 ps as detection unit. The sample was excited along a 10 mm pathlength, and the emission was recorded orthogonally to this along a 10 mm pathlength, while the optical density of the sample was set to *ca.* 0.1 at the excitation wavelength over 10 mm pathlength. The fluorescence quantum yield QY was determined by two different techniques. First, equation 1 was used to calculate the QY with respect to the standard compound $[Ru(bpy)_3](PF_6)_2$ (indirect method) and was then confirmed by a Hamamatsu C9920-02 system equipped with a Spectralon® integrating sphere (direct method). Both methods generated the same fluorescence quantum yields.

$$Q_x = Q_R * \left(\frac{A_R}{A_X}\right) * \left(\frac{E_X}{E_R}\right) \quad (1)$$

Q_X= quantum yield of the investigated compound; Q_R= quantum yield of the reference compound $[Ru(bpy)_3](PF_6)_2$ (Q_A = 0.095)[8]; $A_{R/X}$ = absorbance of the reference compound and the investigated compound at the excitation wavelength, respectively; $E_{R/X}$ = area under the emission curve of the reference compound and the investigated compound, respectively.

Photostability measurements: The photostability was determined by illumination time correlated absorption spectroscopy of **Ru(phenphen)**, **Ru(phenphen)Ru** and **Ru(phenphen)Pt** at 470 nm (one LED-stick (45 ± 5 mW·cm^{-1})) in MeCN at room temperature. Identical starting optical densities (0.19 ± 0.02) at 450 nm for each complex were used.

Electrochemistry: The cyclic voltammograms were carried out in degassed MeCN. As the supporting electrolyte 0.1 M $TBAPF_6$ was used. The measurements were performed with an

Autolab potentiostat PGSTAT204 from Metrohm using a three-electrode configuration. As electrodes a glassy carbon disc with a 3 mm diameter stick (working), a Pt electrode (counter) and a non-aqueous Ag^+/Ag electrode with 0.01 M $AgNO_3$ in MeCN (reference) were utilized. The ferrocenium/ferrocene (Fc^+/Fc) couple was added to the solution after each measurement serving as reference system. All scan rates were 100 mV/s unless otherwise noted.

Transient absorption spectroscopy. The ns to ms transient absorption (TA) was recorded with a in house build transient absorption spectrometer using a streak camera-based detection system as described previously.[9–11] Each sample was excited at 355 nm (10 mJ, *ca.* 10 ns, third harmonic generation of a Nd:YAG laser (10 Hz, Surelite II, Continuum)). As probe pulses a pulsed 150 W Xe-flash lamp (Müller Elektronik-Optik) was used which was focused three times *via* toric mirror optics with foci at: i) before the probe shutter, ii) in the sample, iii) onto the spectrograph's entrance slit. The analysis of the entire probe whitelight pulse was done with a combination of a spectrograph (200is, Bruker) and a streak camera (C7700, Hamamatsu Photonics). Using mechanical shutters, the recording of a sequence of three individual data sets was be achieved: i) an image (D_{FL}) with both flash lamp and laser, ii) an image (D_0) without any incoming light, and iii) an image (D_F) only with the flash lamp. This sequence was repeated 100 times and the corresponding data sets were averaged prior to calculating the final TA as:

$$\Delta\mathrm{OD} = \log\left(\frac{D_\mathrm{F} - D_0}{D_\mathrm{FL} - D_0}\right) \tag{2}$$

The sample (typically 3 mL) was stirred in a cell with a pathlength of 10 mm for pump and 10 mm for probe beams (dimensions: 10 mm × 10 mm × 30 mm, Starna) minimizing any sample degradation due to prolonged intense excitation of the one and the same sample volume. Under these conditions no significant degradation of the photocatalyst was observed.

Analysis of the transient absorption data. The exponential ansatz in the global fit was used to analyse the transient absorption data of each single complex investigated in this study. An in-house written program was used as described previously,[10–14] in which the linear least squares problem in equation (3) is solved.

$$\chi^2 = \|\mathbf{\Delta A} - \mathbf{FB}\|^2 = \mathrm{Min} \tag{3}$$

The time-resolved absorption data are given in matrix ΔA. F is the matrix containing the analytical functions accounting for the temporal changes in the data, *i.e.* exponential decays (convoluted with the instrument response, typically a Gaussian function) and a Gaussian to account for the laser scatter signal within the instruments response. The solution is then given in matrix **B** that contains the to be determined spectra. $\boldsymbol{\chi^2}$ is further optimized by a nonlinear least squares algorithm, in which the rate constants in **F** are optimized. Such a fit results in so-called decay associated difference spectra (DADS in matrix **B**) and their associated optimized rate constants representing the unique result of the global fit. This treatment does not require any model for the kinetics involved in the transient processes. SVD-based rank analysis may determine the number of exponentials prior to the global fit as described in.[15] This DADS only describe the spectral changes observed in the data, *i.e.* positive amplitudes indicate spectral regions that decay with the associated rate constant and negative amplitudes indicate spectral regions that rise with the associated rate constant. Thus, DADS are no species spectra. The model that relates the actual species kinetics to the elementary function needs to be applied

afterwards resulting in species associated spectra (SAS) that allows to extract an actual physical interpretation of the TA data by a model. The appropriateness of the model can be judged by the shape of the SAS in terms of identity with well-known spectra or following physical laws. As this last step does not change the χ^2 value, this procedure has the advantage that all interpretation is performed with the same quality of fit.

Mass spectrometry: High-resolution mass spectrometry (HRMS) were recorded with either a solariX (Bruker Daltonik) equipped with a 7.0 T superconducting magnet and interfaced to an Apollo II Dual ESI/MALDI source or a SSQ 710 spectrometer (Finnigan MAT). Electrospray ionization spectra were recorded with a MAT 95 XL (Thermoquest-Finnigan MAT).

NMR-Experiments: The NMR spectra were recorded on a Bruker AVANCE 400 MHz spectrometer and on a Jeol EX-270 DELTA spectrometer (270 MHz) at ambient temperature, respectively. Chemical shift values (δ) are given in parts per million (ppm) using residual solvent signals (δH = 7.26ppm and δC = 77.16ppm for $CDCl_3$, δH = 1.94 ppm and δC = 118.26 ppm for CD_3CN and δH = 3.31 ppm and δC = 49.05 ppm for MeOD-d_4) as the internal standard.

Crystal-structure analyses: The intensity data for the compounds **Ru(phenphen)** and **phenphen** were collected on a Nonius *Kappa*-CCD diffractometer, using graphite-monochromated Mo-K_α radiation (λ = 0.71073 Å, graphite monochromator) at -123(2)°C for **Ru(phenphen)** and at -140(2)°C for **phenphen**. Data were corrected for Lorentz and polarization effects; for **Ru(phenphen)** a semi-empirical absorption correction was performed on the basis of multiple scans using SADABS 2.06.;[16,17] for **phenphen** the absorption was taken into account on a semi-empirical basis using multiple-scans.[16,18,19]. For **Ru(phenphen)**, the structures were solved by direct methods (SHELXS [10.1107/S0108767390000277]) and refined by full-matrix least squares techniques against F_o^2 (SHELXL-2018/3),[20–22] while for **phenphen**, the structures were solved by intrinsic methods (SHELXT[22]) and refined by full-matrix least squares techniques against F_o^2 (SHELXL-2018[23]). For **Ru(phenphen)** all non-hydrogen atoms were refined anisotropically and all hydrogen atoms were included at calculated positions,[20–22] while for **phenphen** all hydrogen atoms were included at calculated positions with fixed thermal parameters and all non-hydrogen atoms were refined anisotropically.[23]

For **Ru(phenphen)** their isotropic displacement parameters were tied to those of the corresponding carrier atoms by a factor of 1.2 or 1.5. In the molecular structure of **Ru(phenphen)** one of the *t*Bu groups was disordered. Two alternative orientations were refined and resulted in site occupancies of 63(2) and 37(2)% for the atoms C54 – C56 and C54A – C56A, respectively. One of the two PF_6 anions was disordered. Two alternative orientations were refined and resulted in site occupancies of 69.1(7) and 30.9(7)% for the atoms F21 – F26 and F21A – F26A, respectively. This compound crystallized with two molecules of methanol per formula unit, one of which was disordered. Again, two orientations were refined and resulted in site occupancies of 65.0(14) and 35.0(14)% for the affected oxygen atoms O200 and O201, respectively. Similarity restraints and pseudo-isotropic restraints were applied in the refinement of the anisotropic displacement parameters of the disordered atoms. XP (SIEMENS Analytical X-ray Instruments, Inc.) was used for structure representations

The crystal of **phenphen** contains large voids, filled with disordered solvent molecules. The size of the voids is 334 Å^3/unit cell. Their contribution to the structure factors was secured by back-Fourier transformation using the SQUEEZE routine of the program PLATON[24] resulting in 164 electrons/unit cell.

CCDC-2161801 (for **phenphen**) and CCDC-2162101 (for **Ru(phenphen)**) contain the supplementary crystallographic data for this paper. This data can be obtained free of charge *via* http://www.ccdc.cam.ac.uk/products/csd/request/ (or from Cambridge Crystallographic Data Centre, 12 Union Road, Cambridge, CB2 1EZ, UK (fax: ++44-1223-336-033; e-mail: deposit@ccdc.cam.ac.uk).

Hydrogen determination. The amount of generated hydrogen was determined by gas chromatography (GC) on a Bruker Scion SQ with a thermal conductivity detector and argon as carrier gas (column: Restek ShinCarbon ST Micropacked Column, mesh 80/100, 2 m x 0.53 mm I.D., oven temp. 40 °C, flow rate 30 mL min^{-1}, detector temperature 200 °C) using 100 µL of the gas phase. The GC was calibrated by injection of different volumes of a hydrogen/argon mixture with known hydrogen amount.

Turnover number (TON) and turnover frequency (TOF). The turnover number (TON) was calculated according to equation 4 as the amount of hydrogen (in µmol) was divided by the amount of catalyst (in µmol) present in the catalytic mixture.

$$\mathrm{TON_{total}} = \frac{\mathrm{n_{total}(H_2)}}{\mathrm{n(catalyst)}} \tag{4}$$

The turnover frequency (TOF) was calculated according to equation 5 (total TOF) by dividing of the total TON at the respecting time as well as an incremental TOF (equation 6) by dividing the newly formed hydrogen by the time interval.[26]

$$\mathrm{TOF_{total}} = \frac{\mathrm{TON_{total}}}{\mathrm{t_{total}}} \tag{5}$$

$$\mathrm{TOF_{incr}} = \frac{\mathrm{TON_{n+1}} - \mathrm{TON_n}}{\mathrm{t_{n+1}} - \mathrm{t_n}} \tag{6}$$

3. Preparation of solutions for photocatalytic experiments

In a 5 mL GC-vial equipped with a screw cap containing a septum, 300 µL of a 0.7 mM stock solution of **Ru(phenphen)Pt** in dichloromethane were added and evaporated. After that, addition of 2 mL of an acetonitrile, triethylamine, water mixture (v:v:v = 6:3:1) was added under argon atmosphere and the GC vial was sealed with a screw cap. Irradiation of the catalytic mixtures with visible light (LED-stick, λ = 470 ± 20 nm, 45 ± 5 mW cm^{-1}), suitable to excite in the MLCT-band, for defined time intervals (see Figure S7). The power of the LED-stick was determined directly on the surface of the LED-stick as the catalytic solutions are in contact to the LED-stick. The subsequent analysis of the headspace by gas chromatography yields the produced amount of hydrogen.

In a 21 mL schlenk tube, sealed with a standard NS14 rubber septum, 0.14 µmol of **Ru(phenphen)Pt** was added by addition of the respective volume of a dichloromethane/**Ru(phenphen)Pt** stock solution followed by evaporation of the solvent. After that, addition of 7.5 mL of an MeCN, triethylamine, water mixture (v:v:v = 6:3:1) was added under argon atmosphere (glovebox). The tube was finally sealed with a NS14 rubber septum. Irradiation of the catalytic mixtures with visible light (2 LED-sticks, λ = 470 ±20 nm, 45 ±5 $mW \cdot cm^{-1}$ each), suitable to excite the ^{1}MLCT-transition of the complexes, for defined time intervals (see Figure S8). The power of the LED-stick was determined directly on the surface of the LED-stick as the catalytic solutions are in contact to the LED-stick. Analysis of the headspace by gas chromatography, allows the determination of the produced amount of hydrogen.

4. Synthesis

4.1 Synthesis of 5,5'-bis-1,10-phenanthroline (**phenphen)**

Approach 1:

To a degassed solution of 0.172 g anhydrous 2,2'-bipyridine (1.2 mmol, 1 *eq.*) and 0.372 g $Ni(COD)_2$ (1.2 mmol, 1 *eq.*) in 6 mL anhydrous Dimethylformamide (DMF), 0.14 mL anhydrous, degassed 1,5-cyclooctadiene (1.2 mmol, 1 *eq.*) was added in one portion. The resulting suspension was heated at 85 °C for 1 h after which the reaction mixtures turned deep violet. After the addition of 0.26 g (1.0 mmol, 0.8 *eq.*) 5-bromo-1,10-phenanthroline dissolved in 13 mL anhydrous degassed DMF, the reaction was allowed to stir for additional 16 h at 85 °C. Afterwards, the reaction was cooled to room temperature and the solvent was removed under vacuum. Then, the resulting solid was suspended in 20 mL aqueous ammonia (10%) containing 2.0 g KCN. After stirring the suspension for 2 h, filtration, and excessive washing with water yielded a crude residue. The product was extracted with 3x150 mL chloroform (ultrasonic bath) and the organic phase was washed three times with 50 mL water. Subsequently, the organic phase was dried over Na_2SO_4 and celite was added as carrier material for subsequent column chromatography. Removal of chloroform and subsequent column chromatography using deactivated aluminium(III) oxide (activity III) and chloroform/hexane (1:1 – 1:3) as eluent yielded the pure product as white to pale yellow powder. Yield: 69.4 mg (0.19 mmol, 32%).

Approach 2:

To a degassed solution of 2.86 g $NiCl_2 \cdot 6H_2O$ (12.0 mmol, 1.2 *eq.*) and 10.5 g PPh_3 (40.0 mmol, 4 *eq.*) in 80 mL DMF, 0.787 g of zinc powder (12 mmol, 1.2 *eq.*) were added in one portion. The resulting mixture was stirred for 1 h under argon at 60 °C forming a bright red precipitate. After the catalyst had been formed, 2.60 g of 5-bromo-1,10-phenanthroline (10.0 mmol, 1 *eq.*) dissolved in 20 mL degassed DMF, was added. This mixture was stirred for 14 h at 60 °C. Afterwards, this mixture was poured into 180 mL aqueous ammonia (10%) containing 8.0 g KCN and then stirred for 1 h at room temperature. Subsequently, the solids were filtered off and redissolved in chloroform. After washing of the combined organic layers with water and drying with Na_2SO_4, heptane was added to this solution. By the removal of chloroform from this mixture under vacuum a precipitate formed. The crude material was filtered off and purified by chromatography using deactivated aluminium(III) oxide (activity III) and chloroform/hexane 1:3 as eluent. Yield: 315 mg (0.88 mmol, 18%) of pale yellow powder. Recrystallization from ethanol yielded crystals suitable for X-ray diffraction.

^{1}H-NMR ($CDCl_3$, 400 MHz): δ 9.26 (dd, $2H_{(2/2')}$, ^3J = 4.4 Hz, ^4J = 1.6 Hz), 9.19 (dd, $2H_{(9/9')}$, ^3J = 4.4 Hz, ^4J = 1.6 Hz), 8.27 (dd, $2H_{(7/7')}$, ^3J = 8.0 Hz, ^4J = 1.6 Hz), 7.91 (s, $2H_{(6/6')}$), 7.73 (dd, $2H_{(4/4')}$, ^3J = 8.0 Hz, ^4J = 1.6 Hz), 7.69 (dd, $2H_{(8/8')}$, ^3J = 8.0 Hz, ^3J = 4.4 Hz), 7.43 (dd, $2H_{(3/3')}$, ^3J = 8.0 Hz, ^3J = 4.4 Hz).

^{13}C-NMR ($CDCl_3$, 101 MHz): δ 151.04, 150.72, 146.20, 146.11, 136.41, 135.47, 134.79, 128.79, 128.31, 128.20, 123.85, 123.42.

ESI-MS: 359.12205 $[M + H]^+$ (calculated: 359.121914 m/z), 717.22781 $[2M + H]^+$ (calculated: 717.25097 m/z).

Crystal data phenphen: $C_{24}H_{14}N_4$[*], Mr = 358.39 $gmol^{-1}$[*], colourless prism, size 0.096 x 0.066 x 0.054 mm^3, monoclinic, space group C 2/c, a = 16.9786(14), b = 11.1129(9), c = 11.8836(8) Å, β = 121.353(4)°, V = 1914.8(3) $Å^3$, T= -90 °C, Z = 4, $\rho_{calcd.}$ = 1.243 gcm^{-3}[*], μ (Mo-K_α) = 0.76 cm^{-1}[*], multi-scan, transmin: 0.6826, transmax: 0.7456, F(000) = 744, 6286

reflections in h(-21/20), k(-14/14), l(-15/15), measured in the range 3.507° ≤ Θ ≤ 27.469°, completeness Θmax = 99.3%, 2172 independent reflections, R_{int} = 0.0336, 1609 reflections with $F_o > 4\sigma(F_o)$, 127 parameters, 0 restraints, $R1_{obs}$ = 0.0698, wR^2_{obs} = 0.2275, $R1_{all}$ = 0.0887, wR^2_{all} = 0.2441, GOOF = 1.045, largest difference peak and hole: 0.263 / -0.288 e Å^{-3}.

[*] derived parameters do not contain the contribution of the disordered solvent.

4.2 Synthesis of $[(tbbpy)_2Ru(phenphen)](PF_6)_2$ – **Ru(phenphen)**

Approach 1:

To a refluxing solution of 48.4 mg **phenphen** (0.135 mmol, 2 *eq*.) in 3.5 mL ethanol in a three-necked round bottom flask, 1.0 mL water was added. 47.8 mg [$(tbbpy)_2RuCl_2$] (0.0785 mmol, 1 *eq*.) were dissolved in 15.0 mL ethanol and then added dropwise within 5 h to the refluxing solution of **phenphen** using a dropping funnel. To increase the amount of water during the reaction, 3.75 mL H_2O were added dropwise within 5 h also *via* a dropping funnel. After addition of all reagents, the red solution was allowed to stir for further 2 h under reflux. Removal of ethanol under vacuum, followed by addition of 100 mL water, filtration over a glass por 4 frit, and addition of NH_4PF_6 dissolved in a small amount of water yielded the crude product as precipitate containing traces of non-reacted ligand. Further purification could be achieved using column chromatography (Sephadex) with chloroform:acetone:methanol (v:v:v = 160:190:150 mL). The product was obtained as red powder. Yield: 85.8 mg (0.067 mmol, 85%).

Approach 2:

A solution of 125 mg [$(tbbpy)_2RuCl_2$] (0.176 mmol, 1 *eq*.) and 63 mg **phenphen** (0.176 mmol, 1 *eq*.) were dissolved in 90 mL ethanol/water (4:1) and heated to reflux for 2 h in a microwave (150 W). After cooling, ethanol was removed from the solvent under vacuum. The remaining aqueous solution was filtered to remove unreacted material. To this stirred filtrate an aqueous solution of 150 mg NH_4PF_6 dissolved in 3 mL water was added slowly. The resulting precipitate was filtered off and washed with water several times. Afterwards the crude product was redissolved in dichloromethane and the organic layer was dried over Na_2SO_4. Separation of the product mixture could be achieved by column chromatography over silica gel 60 with gradient elution. Using MeCN/water/sat. aqueous KNO_3-solution (250:40:5/v:v:v) two fractions containing **Ru(phenphen)Ru** and **Ru(phenphen)** were obtained. After an additional exchange of the counter ion with NH_4PF_6 and drying the substances under vacuum, pure products were obtained. Yield: 146.6 mg (0.114 mmol, 65%). Purification could also be achieved using column chromatography (Sephadex) with chloroform:acetone:methanol (v:v:v = 160:190:150 mL).

For assignment of the signals, see Figure S13: **^{1}H-NMR (CD_3CN, 400 MHz):** δ 9.23 (td, *J* = 4.0, 3.3, 1.8 Hz, $1H_{(2/9)}$), 9.18 (ddd, *J* = 15.7, 4.3, 1.6 Hz, $1H_{(2/9)}$), 8.64 (ddd, *J* = 8.3, 4.1, 1.2 Hz, $1H_{(4/7)}$), 8.58 – 8.45 (m, $5H_{(3/3'\text{-bpy, }4'/7')}$), 8.37 (s, $1H_{(6'/6')}$), 8.15 (dt, *J* = 5.3, 1.4 Hz, $1H_{(2'/9')}$), 8.12 (s, $0.5H_{(6)}$), 8.08 (dd, *J* = 5.1, 1.1 Hz, $1H_{(2'/9')}$), 8.05 – 7.99 (m, $2H_{(6/3/8)}$), 7.93 – 7.78 (m, $2.5H_{(3/3'/8/8')}$), 7.71 (dd, *J* = 5.9, 3.6 Hz, $2H_{(3/8,\ 6/6'\text{-bpy})}$), 7.68 – 7.60 (m, $1.5H_{(3/8)i}$), 7.58 – 7.42 (m, $4.5H_{(5/5'\text{-bpy, }6/6'\text{-bpy})}$), 7.34 (dt, *J* = 6.2, 2.1 Hz, $1H_{(5/5'\text{-bpy})}$), 7.27 (ddd, *J* = 7.5, 5.8, 2.0 Hz, $1H_{(5/5'\text{-bpy})}$), 1.46 (t, *J* = 1.2 Hz, $9H_{(CH3)}$), 1.43 (s, $9H_{(CH3)}$), 1.41 (t, *J* = 1.0 Hz, $9H_{(CH3)}$), 1.38 (dd, *J* = 2.1, 0.8 Hz, $9H_{(CH3)}$).

^{13}C-NMR (CD_3CN, 101 MHz): δ 163.60, 163.58, 163.48, 163.47, 158.09, 158.04, 157.81, 157.79, 153.47, 153.30, 153.26, 152.61, 152.55, 152.17, 152.08, 152.04, 151.98, 151.80,

151.29, 151.23, 149.11, 148.82, 147.10, 147.05, 138.39, 137.55, 137.42, 137.38, 136.09, 136.07, 135.46, 135.19, 134.48, 134.39, 132.16, 132.08, 131.44, 130.55, 130.48, 130.05, 129.42, 129.12, 129.09, 127.40, 127.38, 126.86, 126.83, 125.55, 125.50, 125.45, 125.45, 125.39, 124.88, 124.85, 124.27, 124.18, 122.48, 122.40, 36.32, 36.29, 36.26, 36.23, 30.44, 30.40.

MALDI-MS: 1141.37589 $[M - PF_6]^+$ (calculated: 1141.37773 m/z).

Crystal data: $[C_{60}H_{62}N_8Ru]^{2+}$, $2[PF_6]^-$, $2(CH_3OH)$, Mr = 1350.27 gmol^{-1}, red-brown plate, size 0.23 x 0.16 x 0.05 mm^3, monoclinic, space group *Cc*, *a* = 28.7888(14), *b* = 12.5327(9), *c* = 18.8750(18) Å, α = 90, β = 114.089(5), γ = 90°, *V* = 6217.0(8) Å^3, *T* = 150(2) K, *Z* = 4, $\rho_{calcd.}$ = 1.443 gcm^{-3}, μ (Mo-K$_\alpha$) = 3.90 cm^{-1}, *F*(000) = 2784, 89373reflections in *h*(-36/36), *k*(-16/16), *l*(-24/24) measured in the range 3.10° $\leq \Theta \leq$ 27.10°, completeness Θ_{max} = 99.8%, 13613 independent reflections, R_{int} = 0.0717, 11804 reflections with $F_o > 4\sigma(F_o)$, 897 parameters, 323 restraints, R_{1obs} = 0.0346, wR_{2obs} = 0.0732, R_{1all} = 0.0473, wR_{2all} = 0.0781, GOOF = 1.076, largest difference peak and hole: 0.420 / -0.288 eÅ^{-3}, absolute structure parameter -0.008(8).[27]

4.3 Synthesis of [(tbbpy)$_2$Ru(phenphen)Ru(tbbpy)$_2$](PF$_6$)$_4$ – **Ru(phenphen)Ru**

A solution of 50 mg $[(tbbpy)_2RuCl_2]$ (0.071 mmol, 2 *eq*.) and 12.6 mg **phenphen** (0.035 mmol, 1 *eq*.) dissolved in 50 mL of ethanol/water (4:1) were heated to reflux for 2 h in a microwave (150 W). After ethanol was removed under vacuum, 20 mL of water were added. After filtration, addition of 3 mL of an aqueous solution of 60 mg NH_4PF_6 induced the formation of a precipitate. Subsequent filtration, washing with excess of water and diethylether, yielded the crude product. Purification was achieved using column chromatography (Sephadex) with chloroform:acetone:methanol (v:v:v = 160:190:150 mL) as solvent. Yield: 75.2 mg (0.034 mmol, 96%) of a red solid.

For assignment of the signals, see Figure S14: **^{1}H-NMR (CD_3CN, 400 MHz):** δ 8.66 (dddd, *J* = 14.4, 8.2, 6.8, 1.3 Hz, $2H_{(4/4'/7/7')}$), 8.53 (ddt, *J* = 14.8, 10.1, 2.2 Hz, $8H_{(3/3'\text{-bpy})}$), 8.40 (d, *J* = 3.9 Hz, $1H_{(6/6')}$), 8.32 (d, *J* = 4.2 Hz, $1H_{(6/6')}$), 8.21 – 8.04 (m, $6H_{(2/2'/9/9'/4/7/4'/7')}$), 7.84 (tdd, *J* = 8.2, 5.3, 4.2 Hz, $2H_{(3/3'/8/8')}$), 7.76 – 7.53 (m, $8H_{(3/3'/8/8',\ 6/6'\text{-bpy})}$), 7.47 (dddd, *J* = 10.4, 9.6, 4.9, 2.9 Hz, $6H_{(5/5'\text{-bpy},\ 6/6'\text{-bpy})}$), 7.35 – 7.25 (m, $4H_{(5/5'\text{-bpy})}$), 1.46 (d, *J* = 1.3 Hz, $9H_{(CH3)}$), 1.45 – 1.43 (m, $9H_{(CH3)}$), 1.41 – 1.37 (m, $18H_{(CH3)}$).

^{13}C-NMR (CD_3CN, 101 MHz): δ 207.45, 163.62, 163.59, 163.51, 163.47, 163.44, 158.06, 158.01, 157.79, 153.86, 153.82, 153.56, 153.51, 153.46, 153.43, 152.61, 152.53, 152.48, 152.19, 152.05, 152.02, 151.96, 149.24, 149.23, 149.11, 148.99, 148.96, 148.94, 137.58, 136.30, 136.23, 135.87, 135.82, 135.60, 135.56, 131.87, 131.80, 131.76, 131.68, 131.32, 131.27, 131.21, 127.55, 127.52, 127.48, 127.06, 126.99, 126.91, 125.60, 125.48, 122.53, 122.49, 122.44, 36.32, 36.24, 30.47, 30.45, 30.41.

MALDI-MS: 2069.61359 $[M - PF_6]^+$ (calculated: 2069.59833 m/z).

4.4 Synthesis of [(tbbpy)$_2$Ru(phenphen)PtCl$_2$](PF$_6$)$_2$ – **Ru(phenphen)Pt**

To a stirred solution of 18 mg (0.043 mmol, 1.1 *eq*.) $[PtCl_2(DMSO)_2]$ dissolved in 30 mL ethanol, 50 mg (0.039 mmol, 1 *eq*.) **Ru(phenphen)** were added. This solution was stirred at 85 °C for 5 h. After this reaction time, 38 mg (0.233 mmol, 6 *eq*.) NH_4PF_6 dissolved in 3 mL water was added. The resulting residue was filtered, washed with water and diethylether. The crude product was dissolved in acetone and filtered *via* a syringe filter. Removal of the solvent

yields the crude product as red solid. Further purification could be achieved using column chromatography (Sephadex) with CAM (chloroform:acetone:methanol; v:v:v = 160:190:150 mL) as solvent. Yield: 59.6 mg (0.038 mmol, 99%) as red solid.

For assignment of the signals, see Figure S15: **^{1}H-NMR (CD_3CN, 400MHz)** δ 9.50 – 9.43 (m, $0.5H_{(2/9)}$), 9.36 (dt, *J* = 15.7, 5.4 Hz, $1.5H_{(2/9)}$), 8.89 (dd, *J* = 13.8, 8.1 Hz, $1H_{(4/7)}$), 8.69 (t, *J* = 7.2 Hz, $1H_{(4'/7')}$), 8.61 (d, *J* = 10.5 Hz, $1H_{(6/6')}$), 8.58 – 8.46 (m, $4H_{(3/3'\text{-bpy})}$), 8.41 (d, *J* = 8.3 Hz, $0.5H_{(4/7)}$), 8.35 (s, $0.5H_{(6/6')}$), 8.31 (dd, *J* = 8.3, 2.7 Hz, $1H_{(2'/9')}$), 8.28 (s, $0.5H_{(6/6')}$), 8.23 (d, *J* = 7.4 Hz, $0.5H_{(4/7)}$), 8.18 (ddd, *J* = 5.0, 3.3, 1.2 Hz, $1H_{(2'/9')}$), 8.12 (dt, *J* = 5.3, 1.5 Hz, $1H_{(2'/9')}$), 7.97 (td, *J* = 7.6, 5.4 Hz, $1H_{(3/8)}$), 7.85 (dt, *J* = 8.2, 4.5 Hz, $1.5H_{(3/3'/8/8')}$), 7.80 – 7.69 (m, $2.5H_{(3/8,\ 6/6'\text{-bpy})}$), 7.65 (t, *J* = 5.9 Hz, $1H_{(6/6'\text{-bpy})}$), 7.62 – 7.56 (m, $1H_{(3'/8')}$), 7.53 – 7.45 (m, $3H_{(5/5'\text{-bpy},\ 6/6'\text{-bpy})}$), 7.36 (dt, *J* = 6.3, 1.4 Hz, $1H_{(5/5'\text{-bpy})}$), 7.29 (td, *J* = 4.1, 2.1 Hz, $1H_{(5/5'\text{-bpy})}$), 1.47 (d, *J* = 1.5 Hz, $9H_{(CH3)}$), 1.44 (s, $9H_{(CH3)}$), 1.42 (s, $9H_{(CH3)}$), 1.39 (d, *J* = 1.9 Hz, $9H_{(CH3)}$).

^{13}C-NMR (CD_3CN, 101MHz) δ 207.44, 163.64, 163.49, 158.09, 158.04, 157.81, 157.79, 153.84, 153.81, 153.49, 153.43, 152.71, 152.64, 152.60, 152.21, 152.12, 152.05, 152.00, 149.97, 149.85, 149.83, 149.55, 149.16, 149.06, 140.48, 140.45, 138.83, 138.62, 137.61, 136.46, 136.32, 136.23, 135.85, 132.28, 132.20, 131.87, 131.77, 131.73, 131.61, 131.55, 131.50, 131.29, 131.23, 130.89, 127.54, 127.50, 127.20, 126.97, 126.91, 125.57, 125.46, 125.43, 122.49, 122.43, 36.30, 36.27, 36.24, 30.45, 30.41.

MALDI-MS: 1407.28207 $[M - PF_6]^+$ (calculated: 1407.28021 m/z), 2959.55324 $[2M - PF_6]^+$ (calculated: 2959.53769 m/z).

5. Supplementary Figures

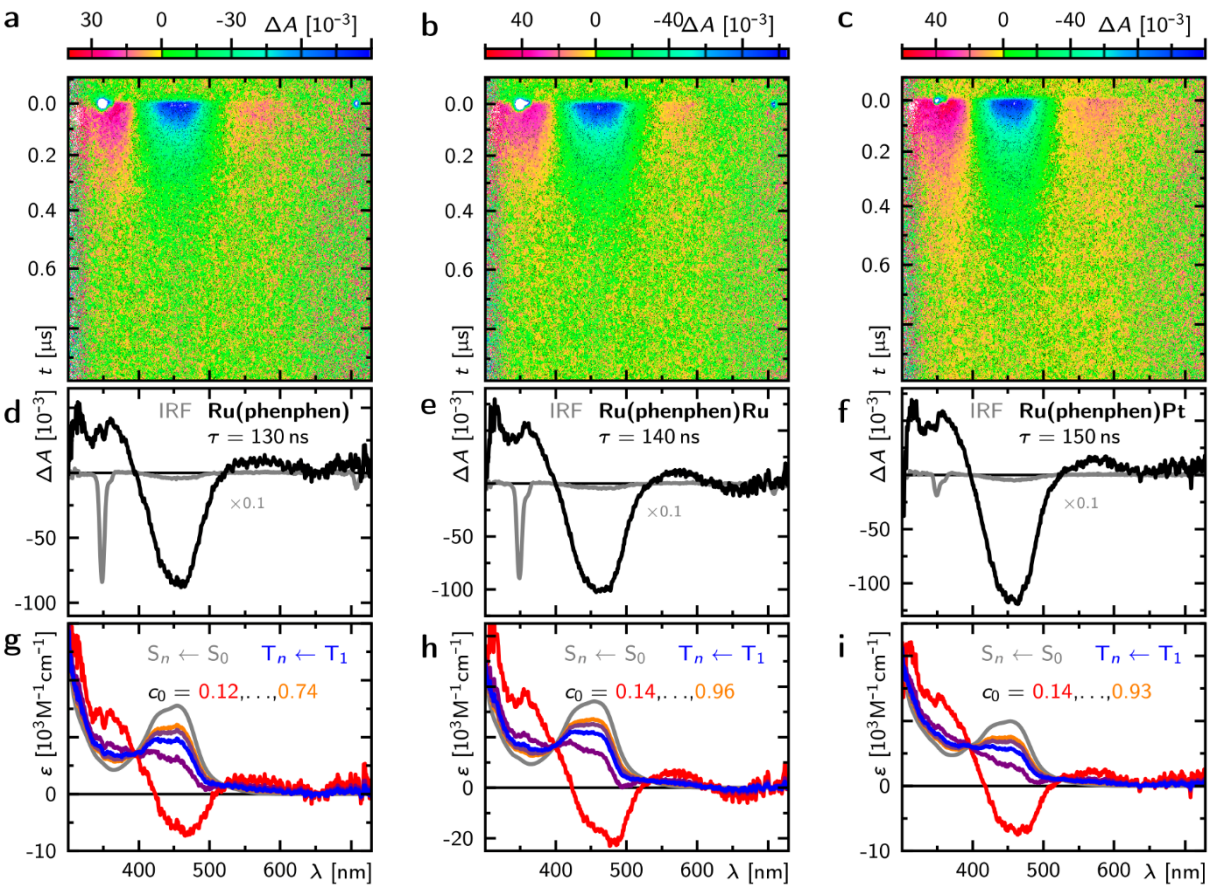

Figure S1. Triplet state dynamics of **Ru(phenphen)** (**a**,**d**,**g**), **Ru(phenphen)Ru** (**b**,**e**,**f**), and **Ru(phenphen)Pt** (**c**,**f**,**i**) in non-degassed MeCN. **a-c**: False colour representation of the time-resolved absorption spectra after excitation at λ_{exc} = 355 nm. **d-f**: Decay associated difference spectra (DADS) from a global bi-exponential fit as indicated, where one lifetime corresponds to the instrument response function and, thus, is denoted as IRF. The resolved lifetime corresponds to the triplet decay back into the ground state in all cases, thus, the DADS shows the triplet absorption minus the ground state absorption. **g-i**: Corresponding species associated spectra (SAS) contributing to the transient absorption data. The triplet spectra ($T_n \leftarrow T_1$ transitions) are determined by varying the ground state contribution, c_0, between lower and upper bounds. At the lower bounds the corresponding spectrum becomes negative and above the contributions of the ground state spectrum ($S_n \leftarrow S_0$ transitions) arise. The ground state S_0 spectrum is plotted in grey for comparison.

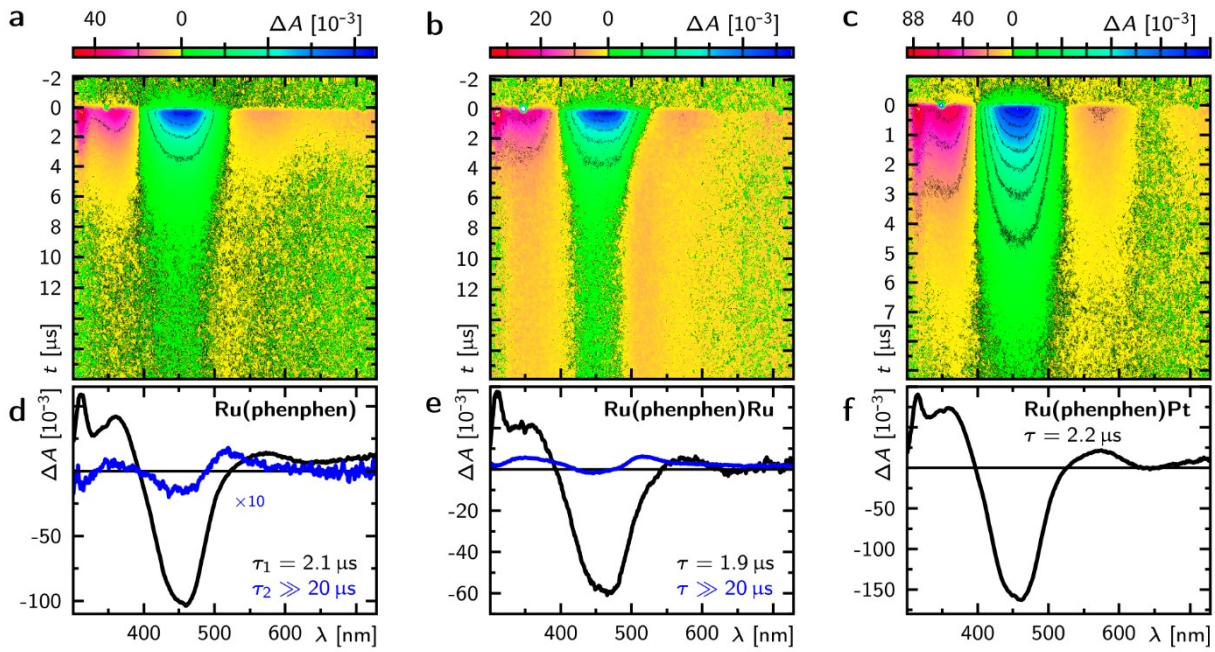

Figure S2. Triplet state dynamics of **Ru(phenphen)** (**a**,**d**), **Ru(phenphen)Ru** (**b**,**e**), and **Ru(phenphen)Pt** (**c**,**f**) in degassed MeCN. **a-c**: False colour representation of the time-resolved absorption spectra after excitation at λ_{exc} = 355 nm. **d-f**: Decay associated difference spectra (DADS) from a global tri-exponential (**d**,**e**) or bi-exponential (**f**) fit as indicated, where one lifetime corresponds to the instrument response function. The IRF is similar to the data shown in Figure S1 and thus is not shown here for simplicity. To note, under these experimental conditions, *i.e.* high transient triplet concentration combined with the absence of molecular oxygen, the triplet lifetime becomes so long that a reaction between the triplets is observed resulting in the formation of an additional photoproduct in cases of **Ru(phenphen)** and **Ru(phenphen)Ru** but not in case of **Ru(phenphen)Pt**.

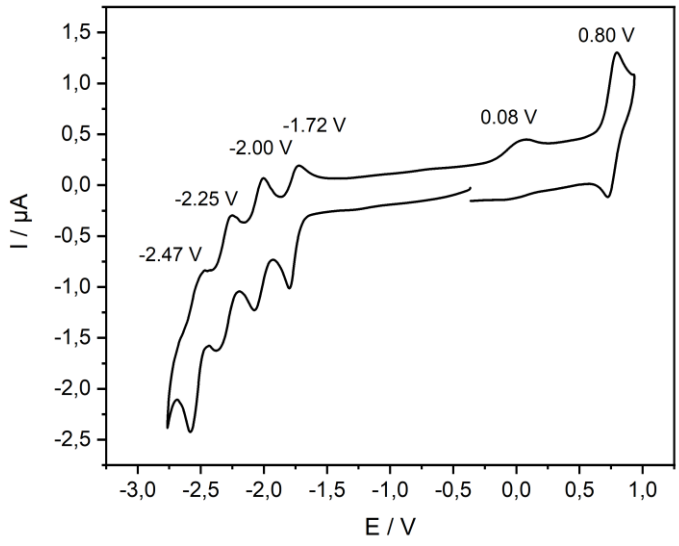

Figure S3. Cyclovoltammogram of **Ru(phenphen)** measured in 0.1 M nBu_4NPF_6 containing MeCN under argon atmosphere, while referencing *vs.* Fc^+/Fc. The measurement was performed using a platinum wire as counter electrode, Ag/AgCl as reference electrode, and a glassy carbon electrode as working electrode.

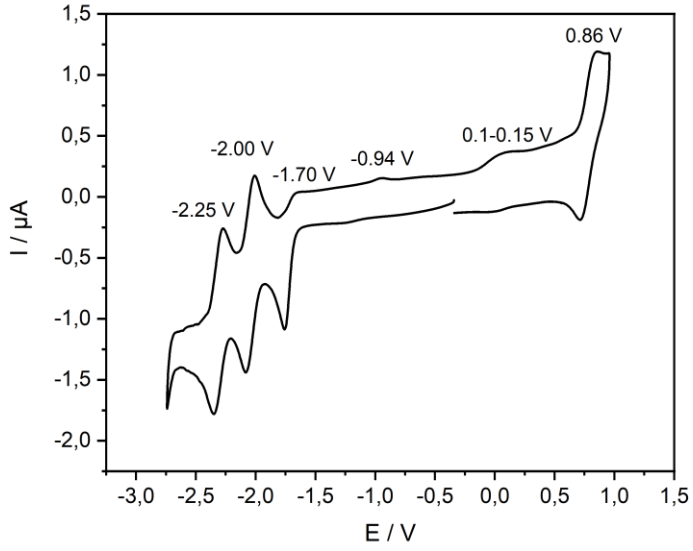

Figure S4. Cyclovoltammogram of **Ru(phenphen)Ru** measured in 0.1 M nBu_4NPF_6 containing MeCN under argon atmosphere, while referencing *vs.* Fc^+/Fc. Measurement was performed using a platinum wire as counter electrode, Ag/AgCl as reference electrode, and a glassy carbon electrode as working electrode.

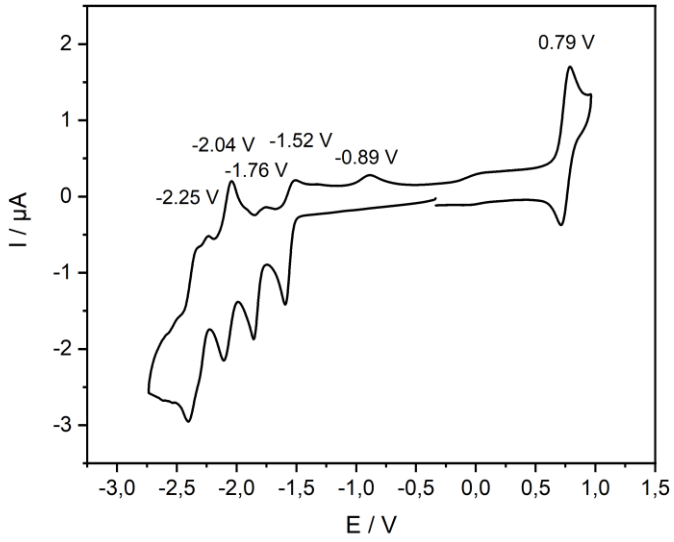

Figure S1. Cyclovoltammogram of **Ru(phenphen)Pt** measured in 0.1 M Bu_4NPF_6 containing MeCN under argon atmosphere, while referencing *vs.* Fc^+/Fc. Measurement was performed using a platinum wire as counter electrode, an Ag/AgCl as reference electrode, and a glassy carbon electrode as working electrode.

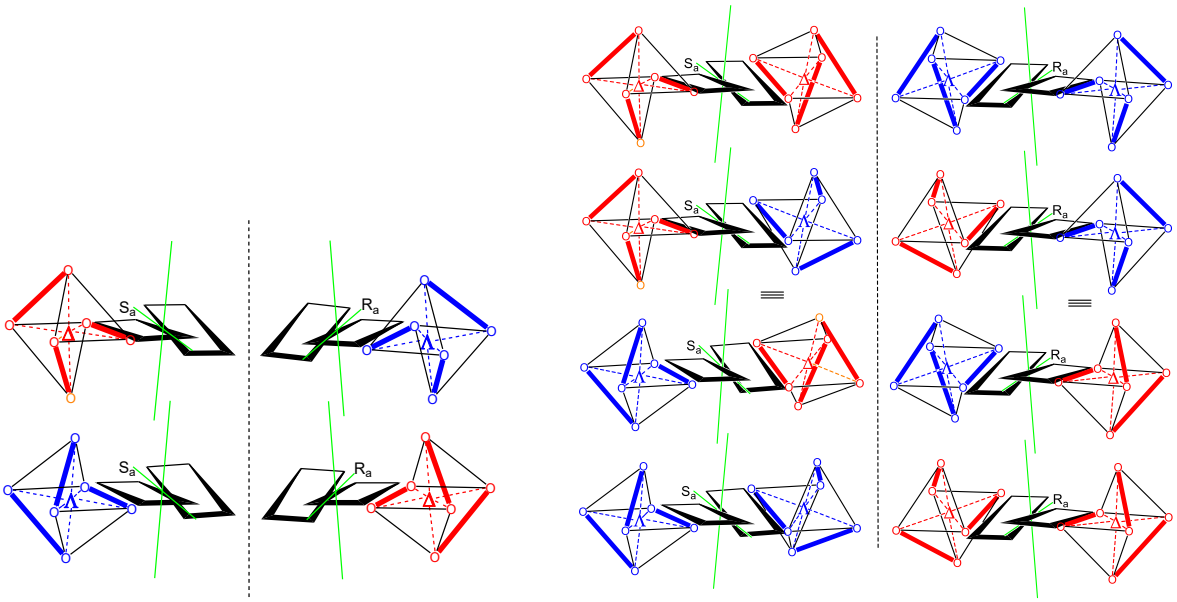

Figure S2. Scheme of all possible stereoisomers (Λ-configuration (blue) and Δ-configuration (red)) of a mono- (left) or homo-binuclear octahedral complex (right), bridged by a ligand with axis chirality (black), like the **phenphen** ligand.

Figure S3. Custom-made microreactor equipped with four air ventilation units and one LED-stick irradiating the samples from the bottom of the GC vial utilized as reaction vessel (λ = 470 ± 20 nm, 45 ± 5 W cm^{-1}).

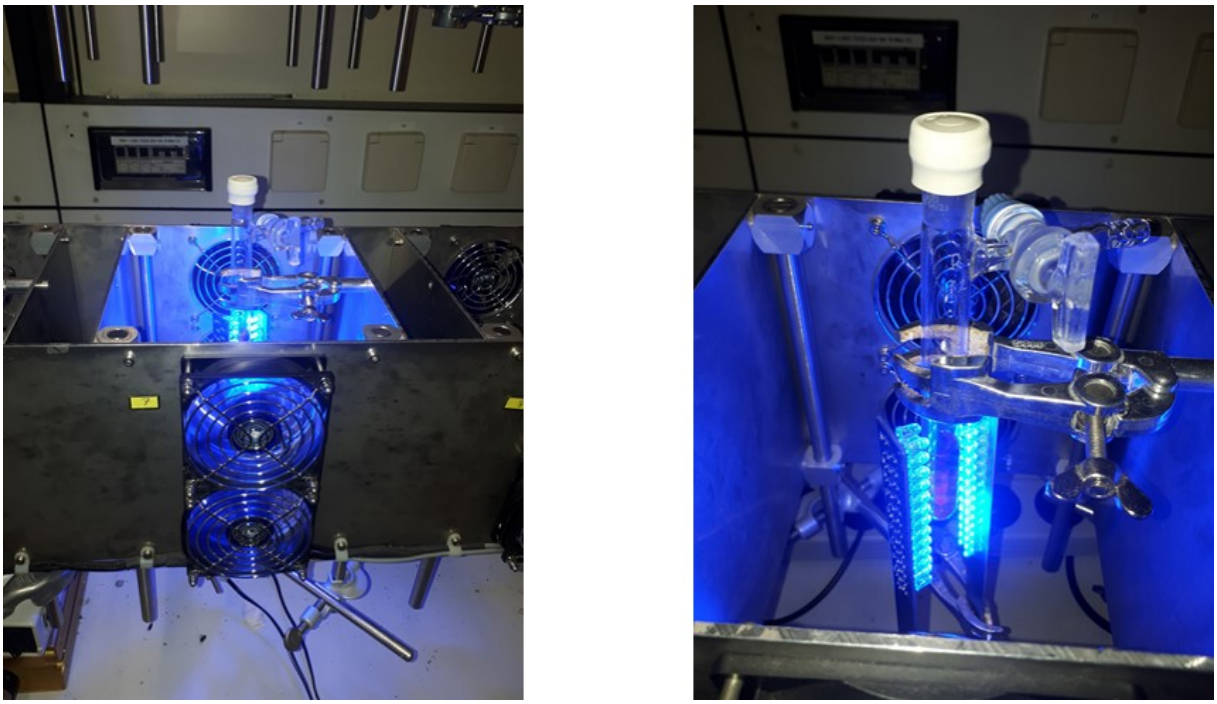

Figure S8. Custom-made photoreactor for schlenk tubes equipped with four air ventilation units and two LED-sticks irradiating the samples from two opposite sides (λ = 470 ± 20 nm, 2 x 45 ± 5 W cm^{-1}).

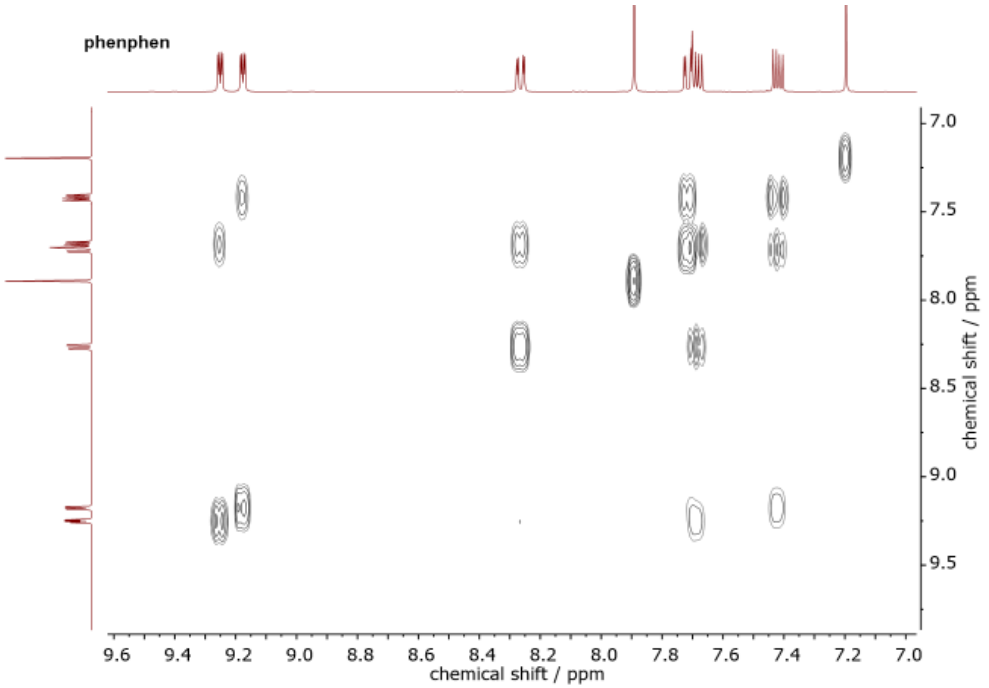

Figure S9. H,H-COSY NMR spectrum (400 MHz) of **phenphen** in deuterated chloroform at room temperature.

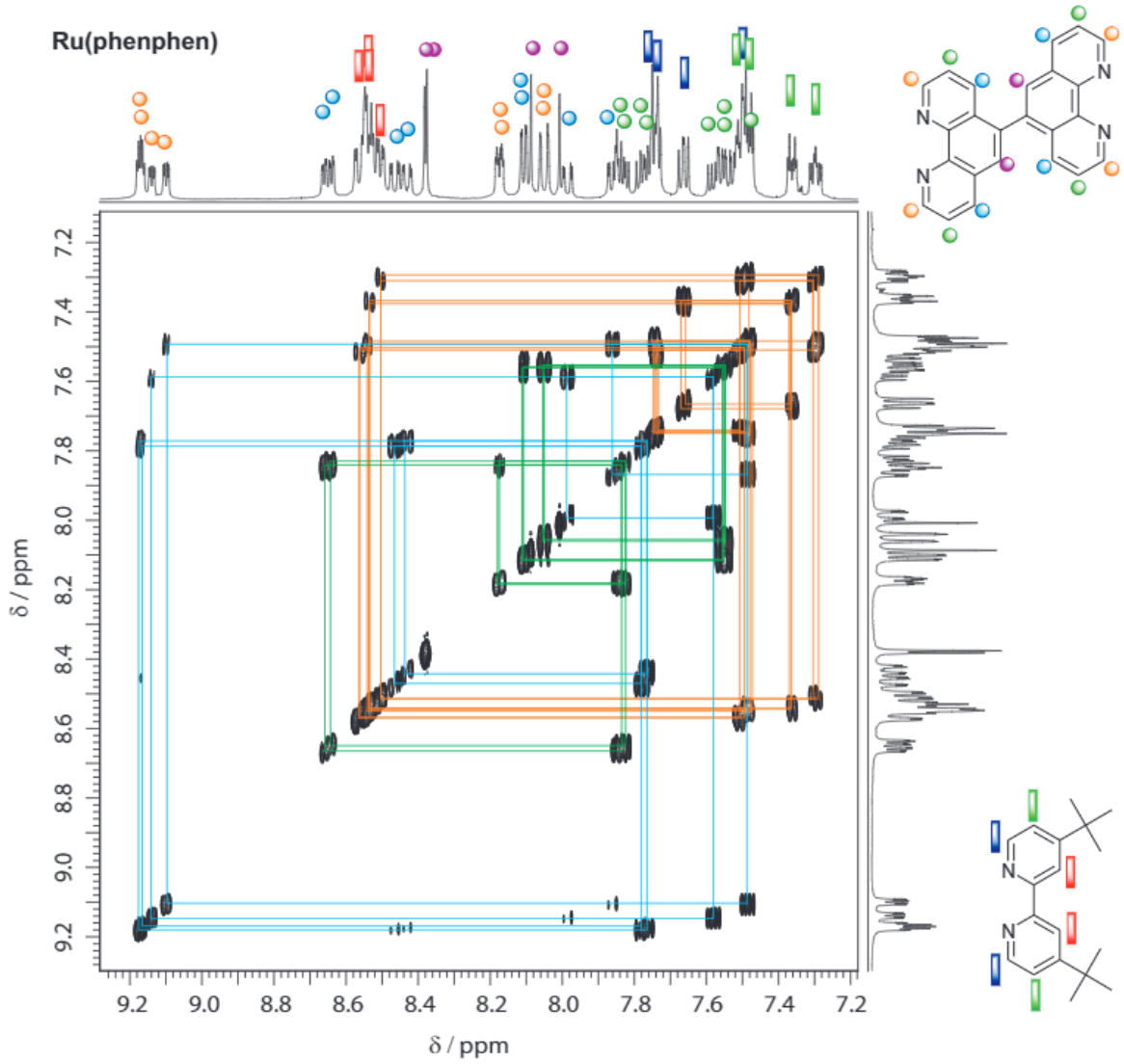

Figure S10. H,H-COSY NMR spectrum (400 MHz) of racemic **Ru(phenphen)** in dichloromethane-d_2 with denoted couplings of the free- (—) and ruthenium coordinated phenanthroline signals (—) plus terminal bipyridine ligand signals (—). The color code of cross-peak correlation and signal assignment in the 1D-spectrum are not related to each other. Color code of the 1D-spectrum signal assignment is represented by the molecular structures depicted on the right.

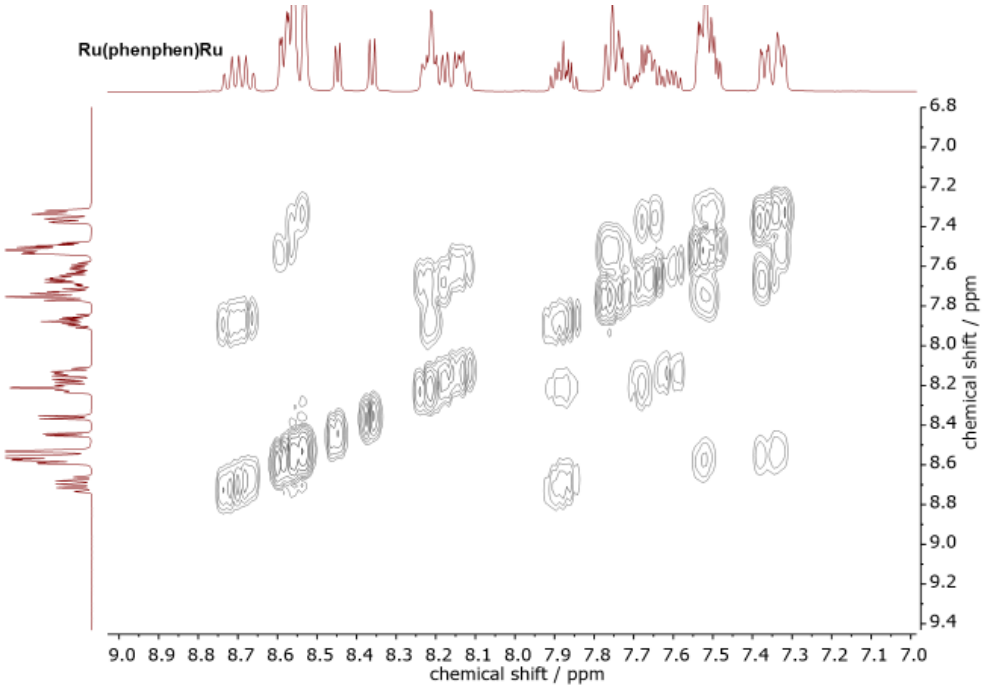

Figure S11. H,H-COSY NMR spectrum (400 MHz) of **Ru(phenphen)Ru** in MeCN-d_3.

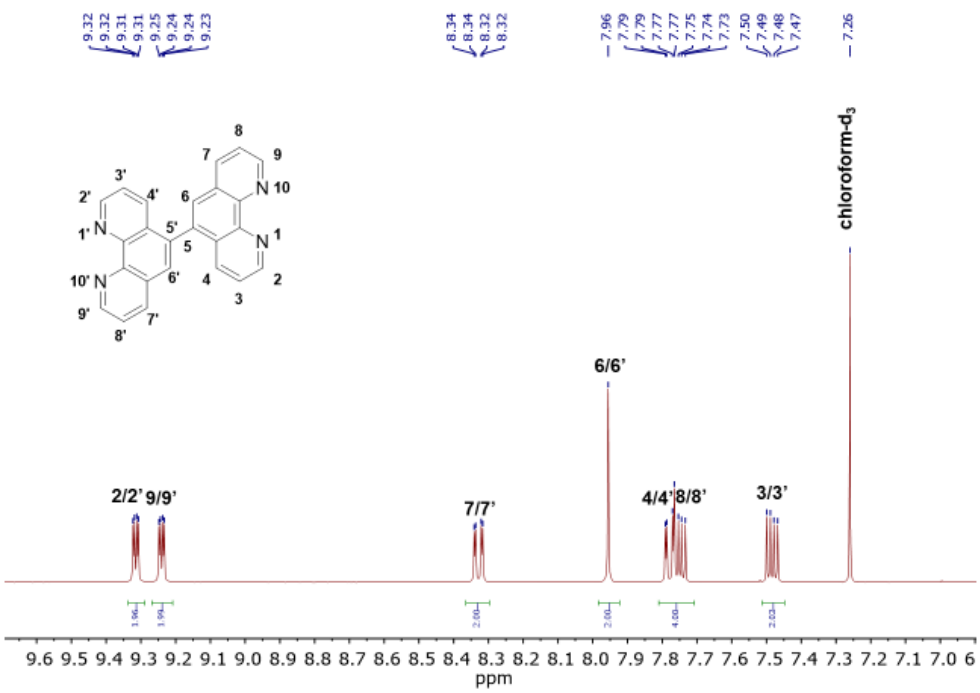

Figure S12. ^{1}H-NMR spectrum of **phenphen** at 400 MHz in chloroform-d_1 at room temperature with signal assignment.

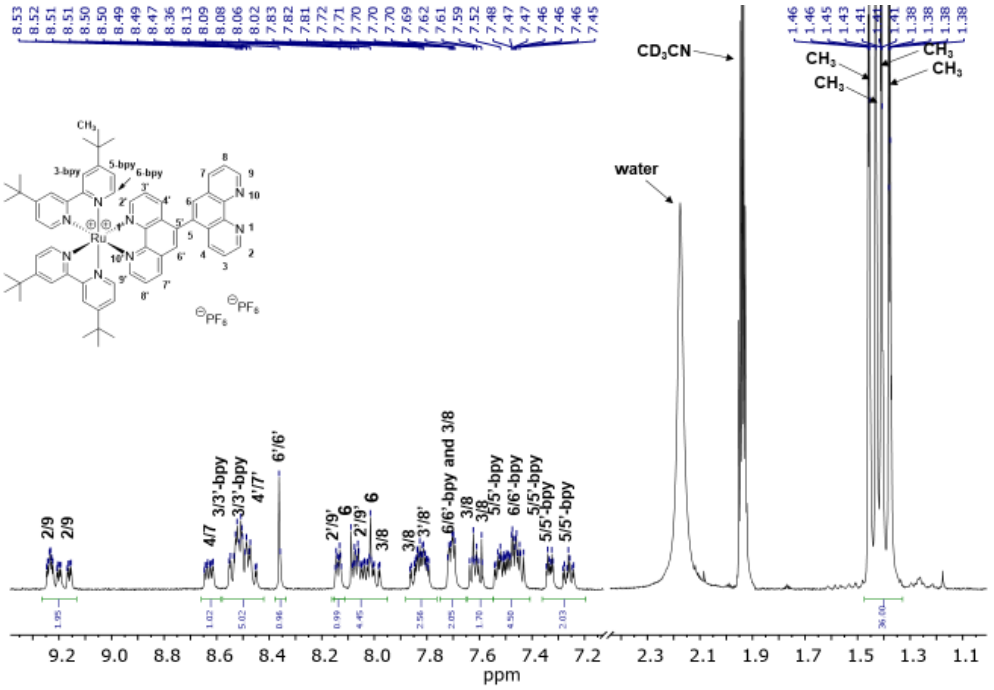

Figure S13. ^{1}H-NMR spectrum of **Ru(phenphen)** at 400 MHz in MeCN-d_3 at room temperature with signal assignment.

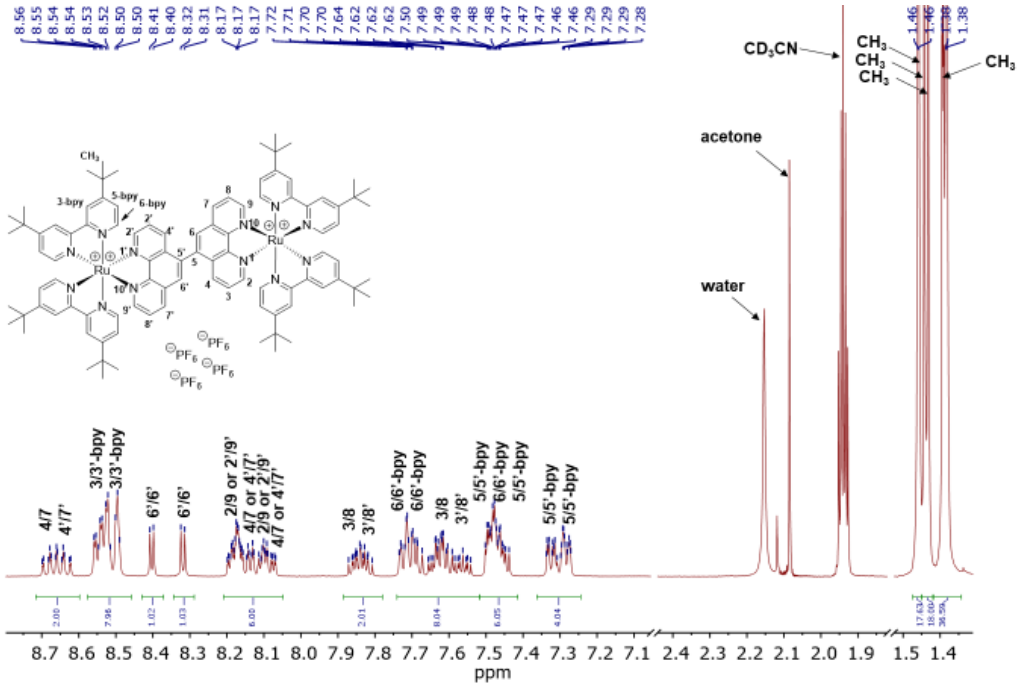

Figure S14. ^{1}H-NMR spectrum of **Ru(phenphen)Ru** at 400 MHz in MeCN-d_3 at room temperature with signal assignment.

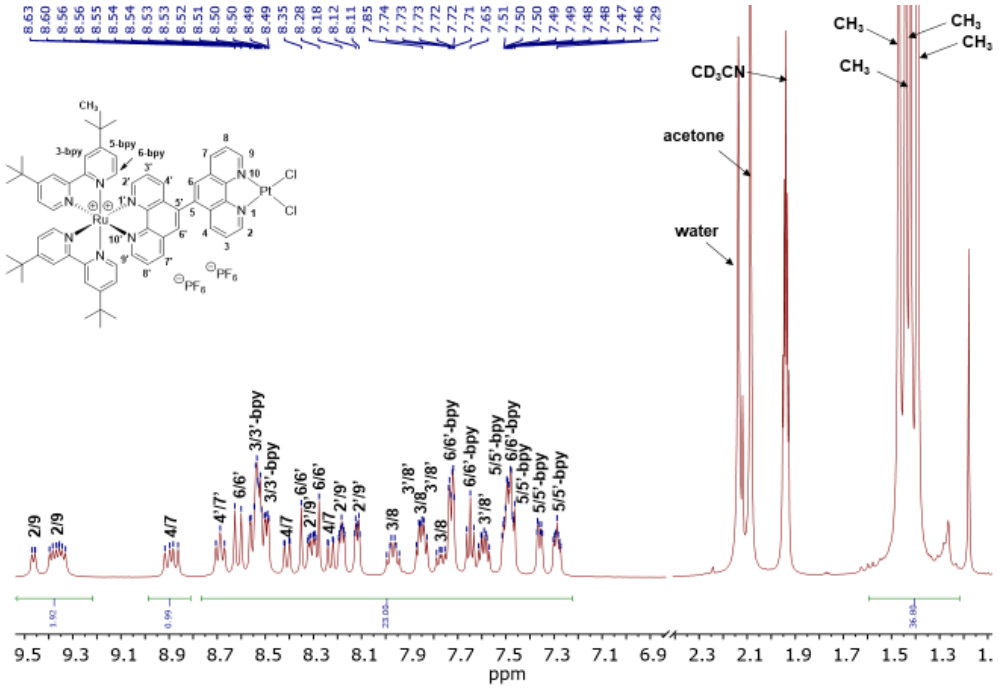

Figure S15. ^{1}H-NMR spectrum of **Ru(phenphen)Pt** at 400 MHz in MeCN-d_3 at room temperature with signal assignment.

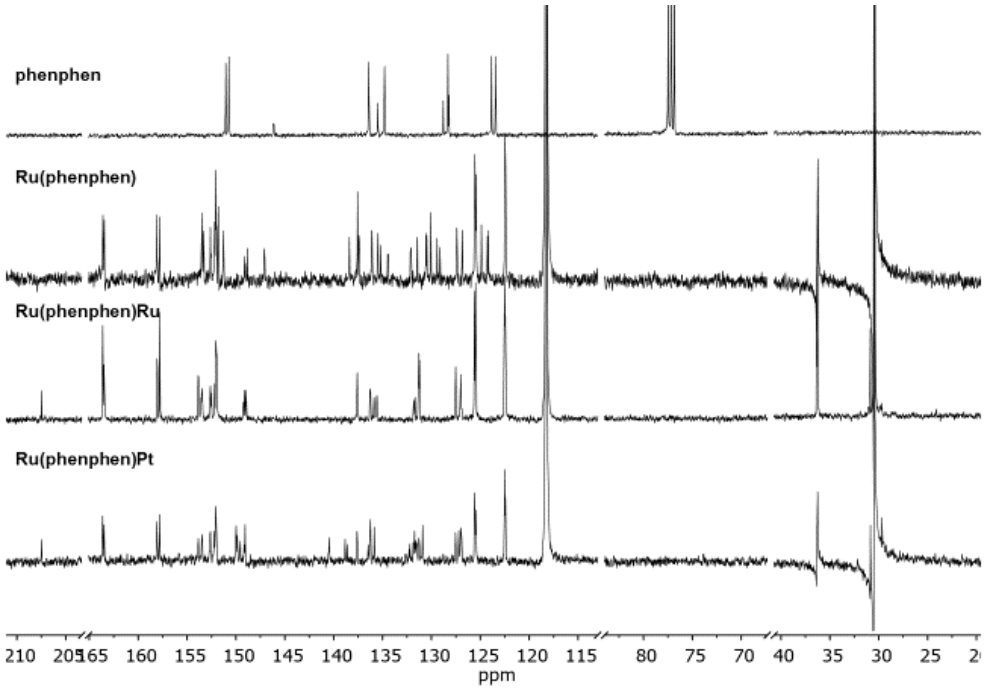

Figure S16. ^{13}C-NMR spectrum of **phenphen** (1st, $CDCl_3$), **Ru(phenphen)** (2nd, CD_3CN), **Ru(phenphen)Ru** (3rd, CD_3CN), and **Ru(phenphen)Pt** (4th, CD_3CN) at 101 MHz at room temperature.

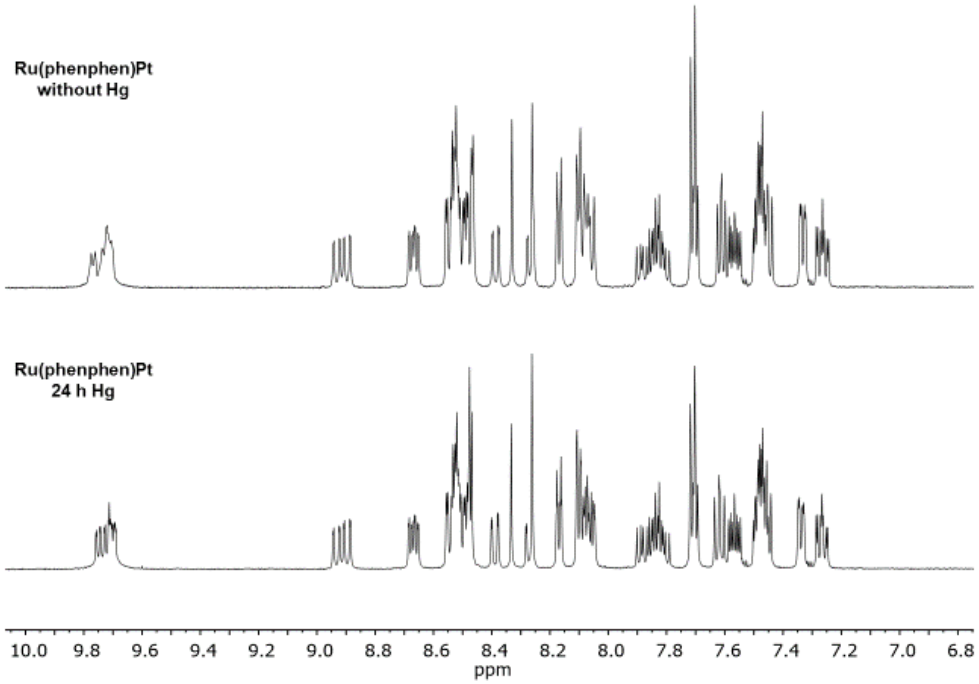

Figure S17. ^{1}H-NMR spectrum of **Ru(phenphen)Pt** without (top) and after addition of mercury and stirring overnight (bottom) in deuterated MeCN (measurement at 400 MHz at room temperature).

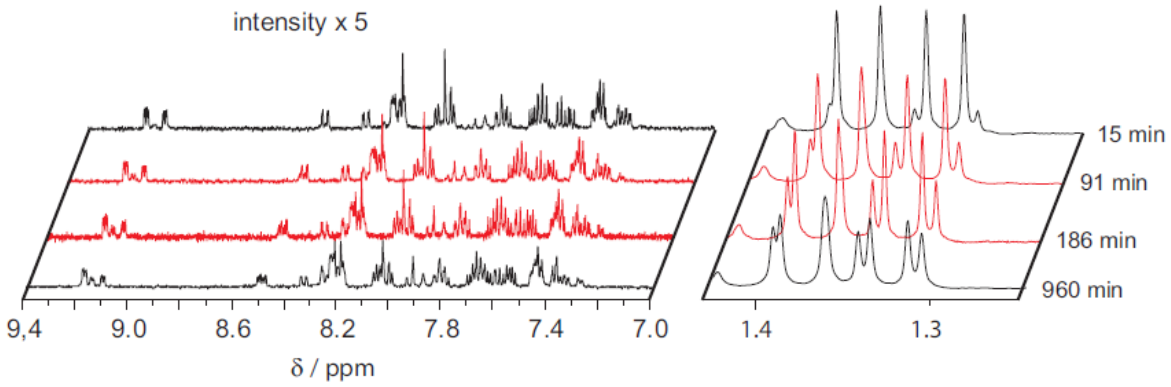

Figure S18. Changes of the ^{1}H-NMR spectrum of **Ru(phenphen)** during 16 h after dissolving the diastereomerically pure complex exhibiting (Δ,Ra)/(Λ,Sa)-configuration (single crystal). Formation of the racemic mixture of rotamers is observed.[28]

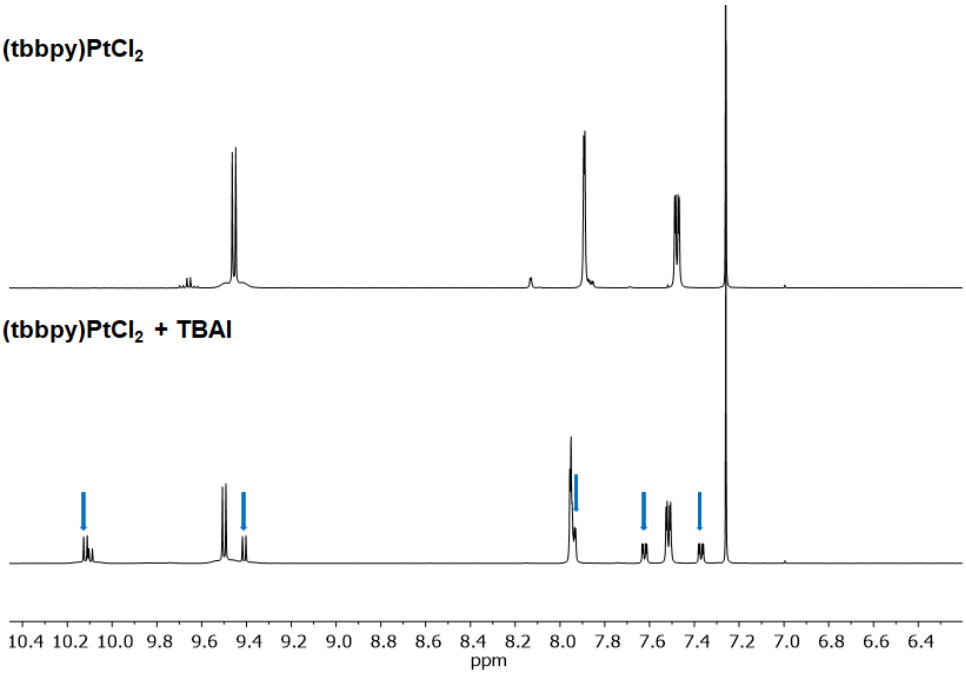

Figure S19. ^{1}H-NMR spectrum of [(tbbpy)PtCl$_2$] without (top) and with addition of an excess of TBAI after 24 h without irradiation in deuterated chloroform at room temperature with 400 MHz. New signals marked in blue indicated the formation of a new species. Small signals in the upper spectrum are impurities of tbbpy.

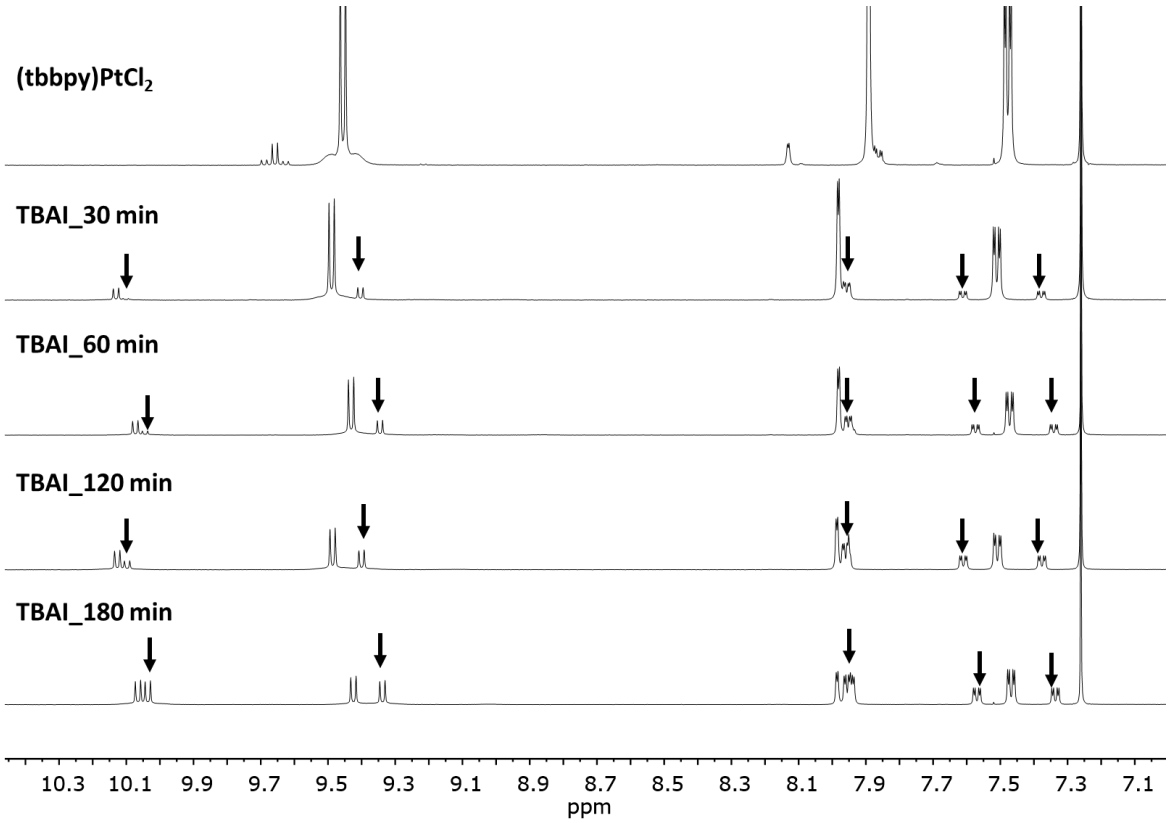

Figure S20. ^{1}H-NMR spectrum of [(tbbpy)PtCl$_2$] without (top) and with addition of an excess of TBAI after 30, 60, 120 and 180 min without irradiation in deuterated chloroform at room temperature with 400 MHz. New signals marked in black indicate the formation of a new species. The slight shifts of the proton signals are attributed to the slightly varying concentrations of TBAI altering the surrounding chemical environment.

Table S1. Formation of the newly formed species in Figure 20 after addition of 200 *eq*. TBAI to [(tbbpy)$PtCl_2$]. The build-up was calculated as the ratio between the total integrals of all resonances of the aromatic proton signals (integral of 6 protons at 7.33 ppm and 7.6 ppm) of the newly formed species with respect to the starting Pt-complex at around 7.5 ppm.

Reaction time	7.33 ppm	7.60 ppm
0 min	0	0
30 min	0.15	0.15
60 min	0.27	0.27
120 min	0.42	0.43
180 min	0.47	0.47

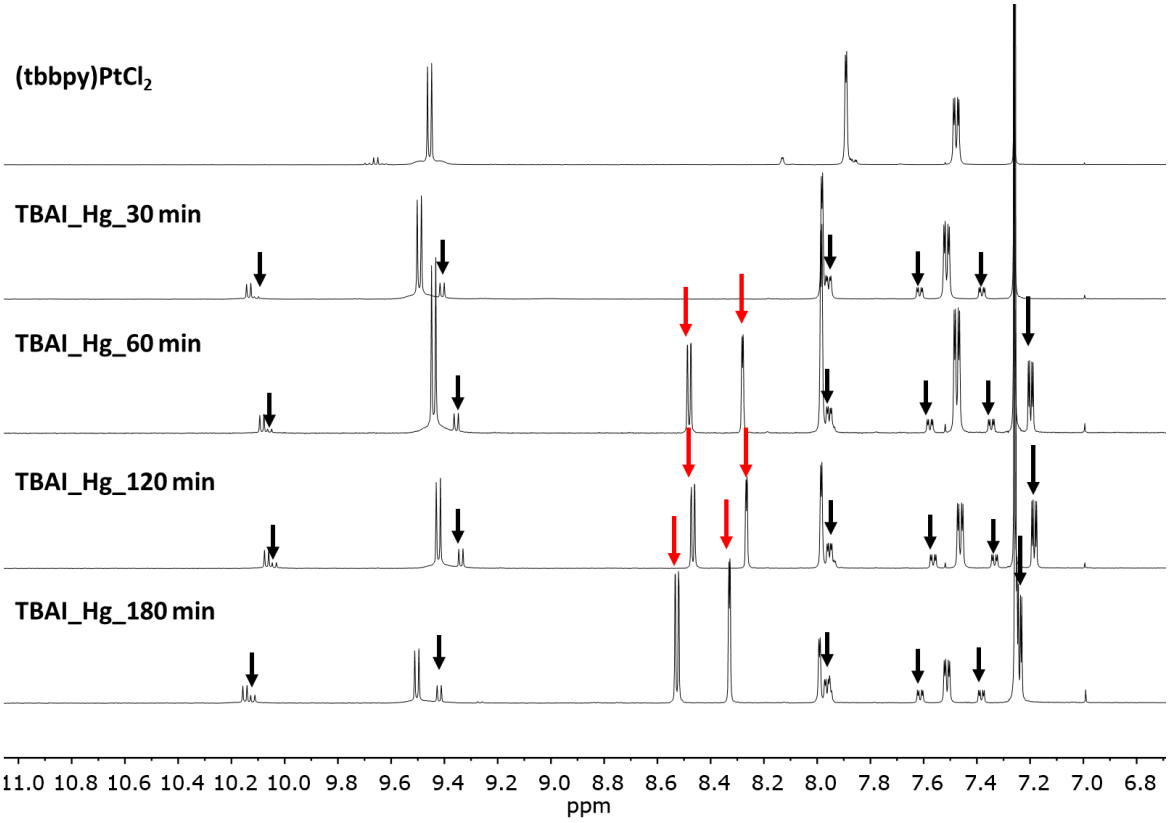

Figure S21. ^{1}H-NMR spectrum of [(tbbpy)$PtCl_2$] without (top) and with addition of an excess of TBAI and three drops of Hg after 30, 60, 120 and 180 min without irradiation in deuterated chloroform at room temperature with 400 MHz. New signals marked in black indicate the formation of the new species as described in Figure S20. The new arising signals marked in red can be assigned to the free ligand tbbpy indicating the instability of the [(tbbpy)$PtCl_2$] complex in the presence of elemental mercury. The slight shifts of the proton signals are attributed to the slightly varying concentrations of TBAI altering the surrounding chemical environment.

Table S2. Formation of newly formed species in Figure 21 after addition of 200 *eq*. TBAI and three drops of Hg to [(tbbpy)$PtCl_2$]. The build-up was calculated as the ratio between the total integrals of all resonances of the aromatic proton signals (integral of 6 protons at 7.33 ppm, 7.6 ppm, 8.27 ppm, and 8.48 ppm) of the newly formed species with respect to the starting Pt-complex at around 7.5 ppm.

Reaction time	7.33 ppm	7.60 ppm	8.27 ppm	8.48 ppm
0 min	0	0	0	0
30 min	0.17	0.18	0	0
60 min	0.14	0.14	0.43	0.44
120 min	0.23	0.24	0.72	0.73
180 min	0.22	0.23	1.50	1.51

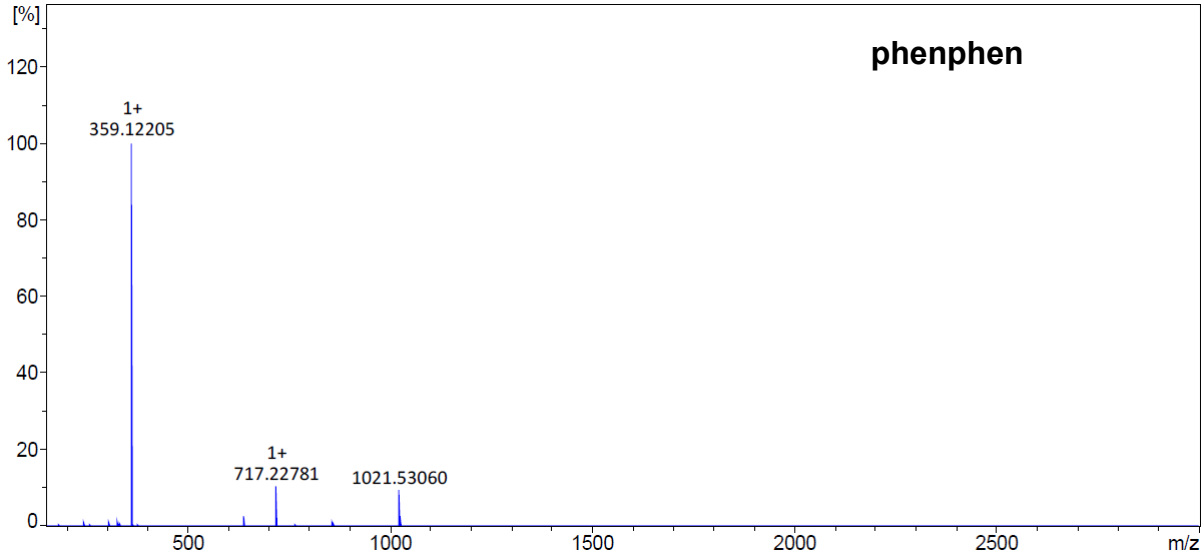

Figure S22. High-resolution ESI-MS spectra of **phenphen** ($[M + H]^+$ calculated: 359.12205 m/z).

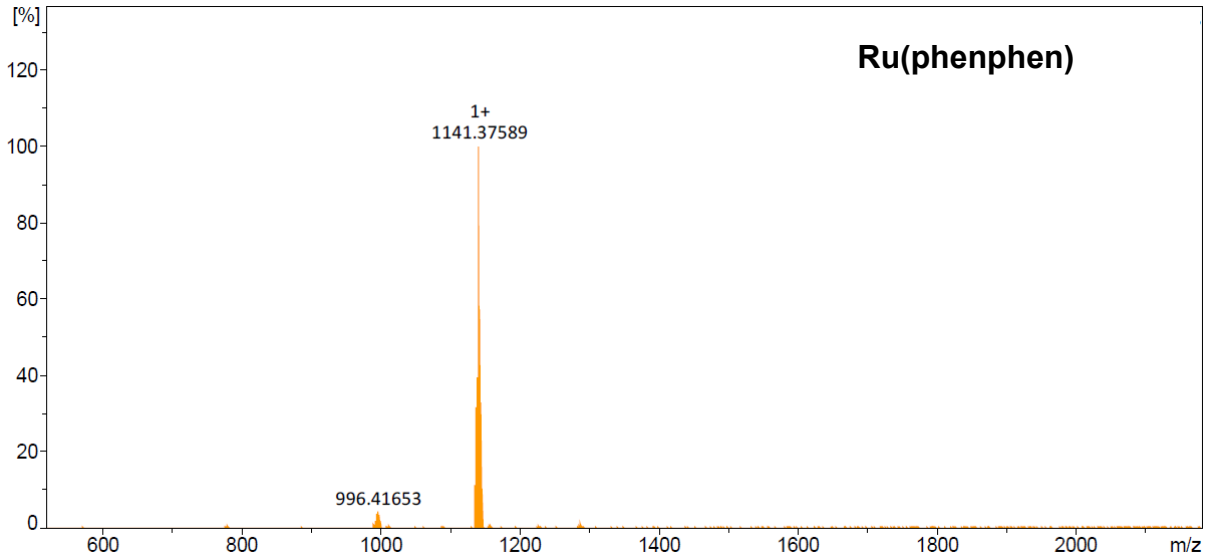

Figure S23. High-resolution MALDI-MS spectra of **Ru(phenphen)** ($[M – PF_6]^+$ calculated: 1141.37773 m/z).

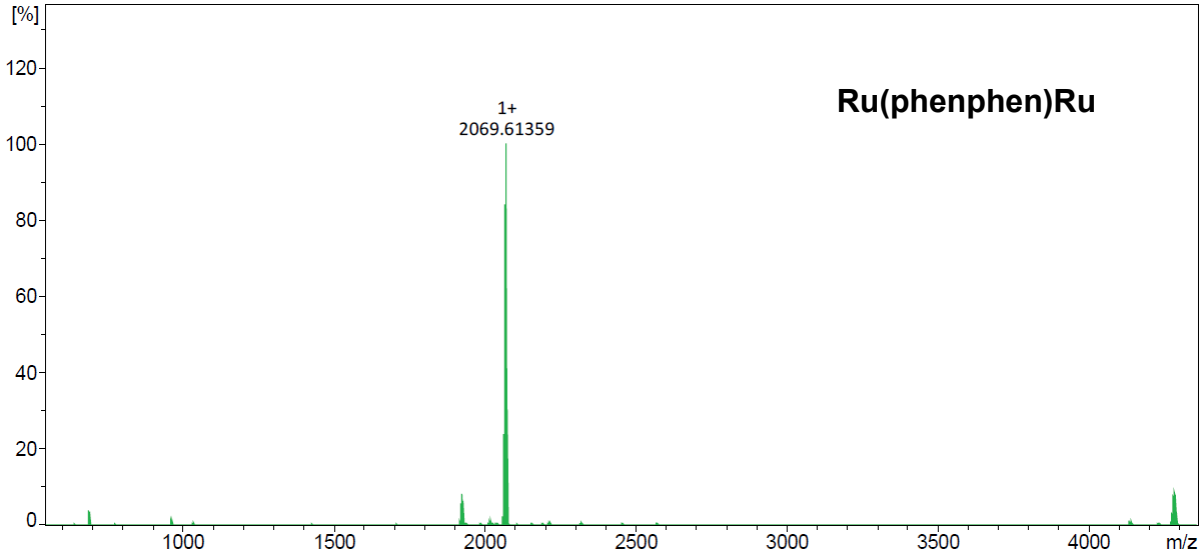

Figure S24. High-resolution MALDI-MS spectra of **Ru(phenphen)Ru** ($[M - PF_6]^+$ calculated: 2069.59833 m/z).

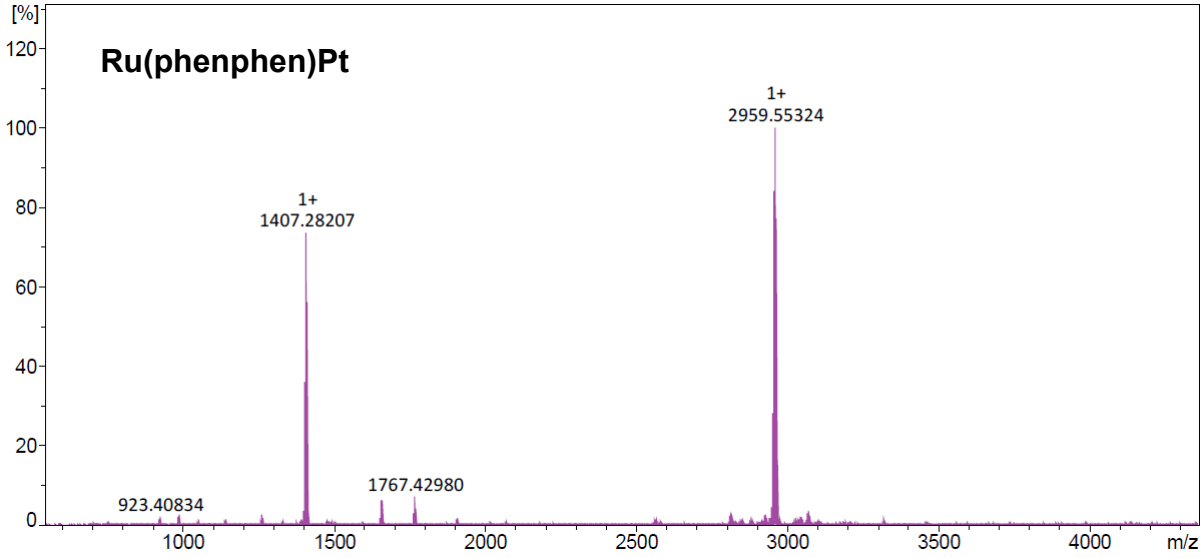

Figure S25. High-resolution MALDI-MS spectra of **Ru(phenphen)Pt** ($[M - PF_6]^+$ calculated: 1407.28021 m/z; $[2M - PF_6]^+$ calculated 2959.53769 m/z).

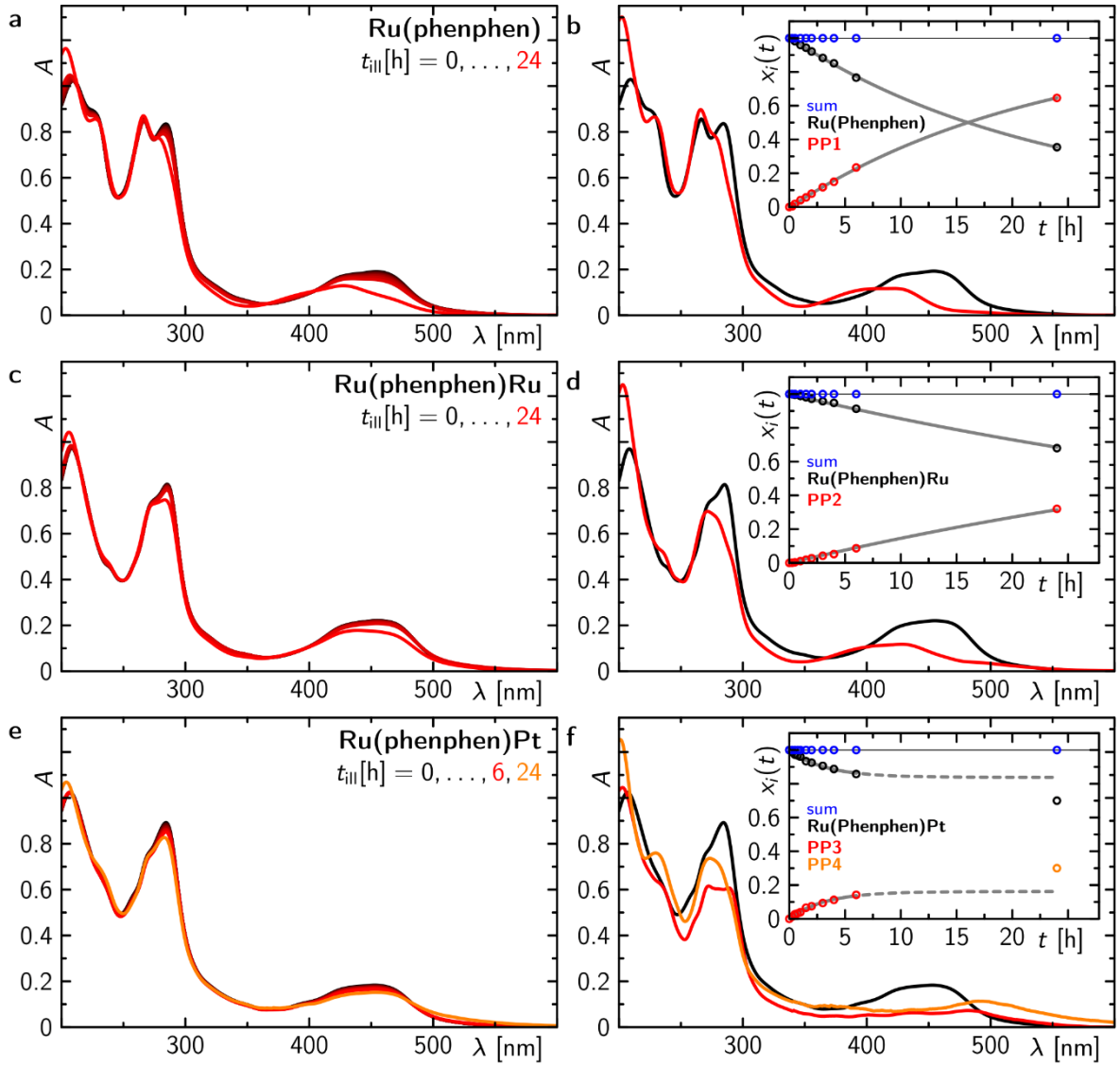

Figure S26. Sequence of stationary absorption spectra and the corresponding concentration-time profiles obtained after stepwise illumination of **Ru(phenphen)** (**a**-**b**), **Ru(phenphen)Ru** (**c**-**d**), and **Ru(phenphen)Pt** (**e**-**f**) at 470 nm (one LED-stick (45 ± 5 mW·cm^{-1})) in MeCN at room temperature. Identical starting optical densities (0.19 ± 0.02) at 450 nm for each complex were used.

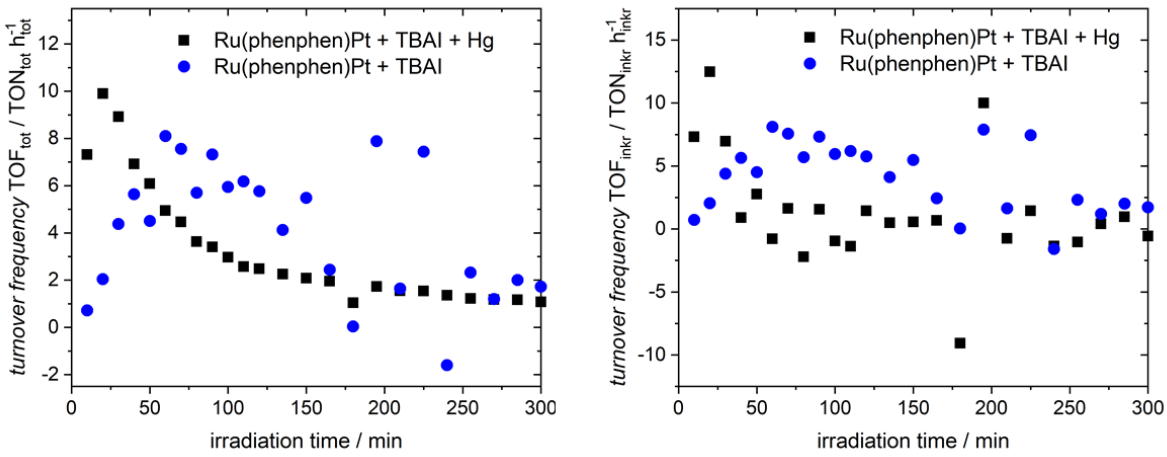

Figure S27. Turnover frequency TOF of **Ru(phenphen)Pt** with addition of TBAI and/or mercury in 6:3:1 (v:v:v) MeCN:TEA:H_2O at defined irradiation times. On the left side, the total TOF was calculated by equation 5 while on the right side, the incremental TOF was calculated according to equation 6.

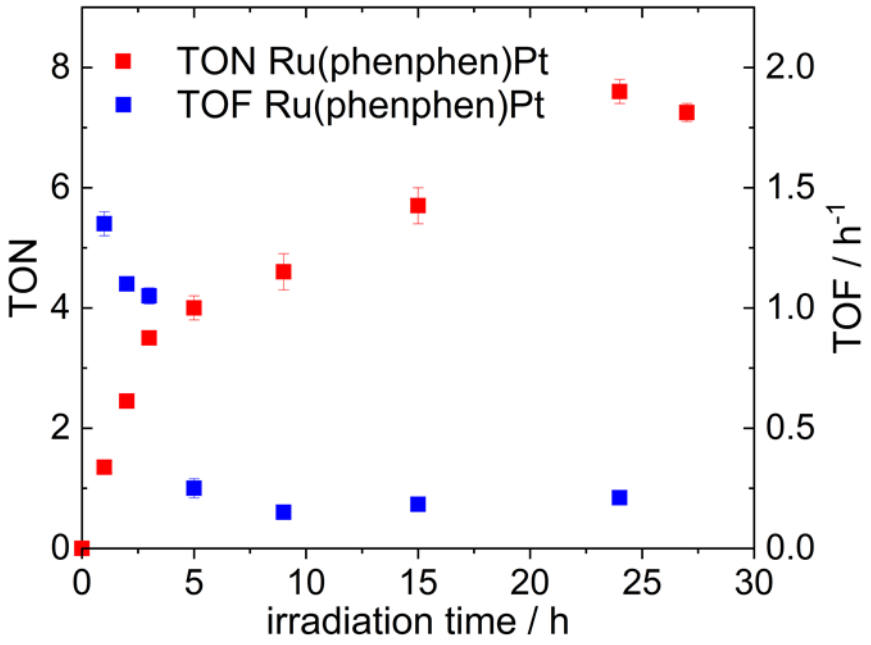

Figure S28. Light-induced hydrogen evolution by **Ru(phenphen)Pt** in 6:3:1 MeCN:TEA:H_2O (6:3:1, v:v:v) under Ar atmosphere, irradiated at 470 ± 20 nm with one LED-stick (45 ± 5 mW cm^{-1}) in a GC vial. The produced amount of molecular hydrogen was determined by gas chromatographic analysis of the headspace. Data points represent the average of n = 2 individual measurements.

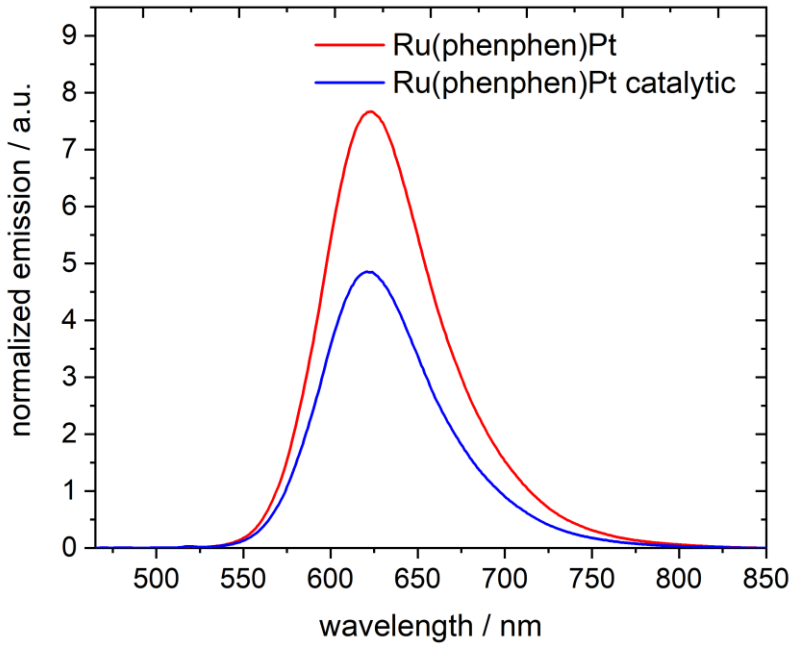

Figure S29. Normalized emission spectrum (divided by the absorbance at 450 nm) of **Ru(phenphen)Pt** in Ar-saturated MeCN (red) and under Ar-saturated catalytic conditions (V_{MeCN}:V_{TEA}:V_{H2O} = 6:3:1). The system was excited at 450 nm. A luminescence quenching by 36% was observed.

Table S3. TONs of **Ru(phenphen)Pt** with and without Hg after defined irradiation times under Ar-saturated, catalytic conditions (6:3:1 = v:v:v, MeCN:TEA:H_2O, 70 µM). Turning off the light for 24 h stops catalysis. Notably, reirradiation starts the catalysis again. In case of the addition of Hg, no further catalysis was observed due to complete reaction of Hg with generated platinum colloids.

Irradiation times	**Ru(phenphen)Pt TON**	**Ru(phenphen)Pt with Hg TON**
0 h	0	0
24 h	11.68	1.59
48 h	22.26	2.67
light turned off		
72 h	21.72	2.54
light turned on again		
96 h	30.99	2.31
168 h	54.22	2.46

6. Crystallography

Table S4. Crystal data and structure refinement for FO3698_**phenphen**.

Identification code	FO3698
Empirical formula	$C_{24}H_{14}N_4$
Moiety formula	$C_{24}H_{14}N_4$ [+ solvent]
Formula weight	358.39
Temperature/K	183(2) K
Wavelength, radiation type	0.71073Å, MoK_α
Diffractometer	KappaCCD
Crystal system	Monoclinic
Space group name	C 2/c, (No. 15)
a	16.9786(14) Å
b	11.1129(9) Å
c	11.8836(8) Å
α	α = 90°
β	β = 121.353(4)°
γ	γ = 90°
Volume	1914.8(3) $Å^3$
Number of reflections	6286
and range used for lattice parameters	3.51° <=θ<= 27.47°
Z	4
Density (calculated)	1.243 Mg/m^3
Absorption coefficient	0.076 mm^{-1}
Absorption correction	Semi-empirical from equivalents
Max. and min. transmission	0.7456 and 0.6826
F(000)	744
Crystal size, colour and form	0.096 x 0.066 x 0.054 mm^3, colourless prism
Theta range of data collection	3.507 to 27.469°
Index ranges	-21<=h<=20, -14<=k<=14, -15<=l<=15
Number of reflections:	
collected	6286
independent	2172 [R(int) = 0.0336]
observed [I>2sigma(I)]	1609
Completeness to theta = 25.2°	99.3 %
Refinement method	Full-matrix least-squares on F^2
Data / restraints / parameters	2172 / 0 / 127
Goodness-of-fit on F^2	1.045
Final R indexes [I>=2σ (I)]	R_1 = 0.0698, wR_2 = 0.2275
Final R indexes [all data]	R_1 = 0.0887, wR_2 = 0.2441
Largest diff. peak/hole	0.263 and -0.288 e $Å^{-3}$

Table S5. Bond lengths [Å] and angles [°] for FO3698_**phenphen**.

N1-C1	1.323(3)	C6-C5-C4	119.59(18)
N1-C12	1.363(3)	C6-C5-C5#1	120.27(15)
N2-C10	1.325(3)	C4-C5-C5#1	120.14(14)
N2-C11	1.360(3)	C5-C6-C7	121.75(18)
C1-C2	1.395(3)	C5-C6-H6A	119.1
C1-H1A	0.9500	C7-C6-H6A	119.1
C2-C3	1.375(3)	C11-C7-C8	117.79(18)
C2-H2A	0.9500	C11-C7-C6	119.86(17)
C3-C4	1.410(3)	C8-C7-C6	122.31(19)
C3-H3A	0.9500	C9-C8-C7	118.99(19)
C4-C12	1.411(3)	C9-C8-H8A	120.5
C4-C5	1.446(3)	C7-C8-H8A	120.5
C5-C6	1.359(3)	C8-C9-C10	118.98(19)
C5-C5#1	1.492(4)	C8-C9-H9A	120.5
C6-C7	1.433(3)	C10-C9-H9A	120.5
C6-H6A	0.9500	N2-C10-C9	124.2(2)
C7-C11	1.410(3)	N2-C10-H10A	117.9
C7-C8	1.412(3)	C9-C10-H10A	117.9
C8-C9	1.368(3)	N2-C11-C7	122.81(18)
C8-H8A	0.9500	N2-C11-C12	118.15(18)
C9-C10	1.397(3)	C7-C11-C12	119.03(18)
C9-H9A	0.9500	N1-C12-C4	122.65(18)
C10-H10A	0.9500	N1-C12-C11	117.85(18)
C11-C12	1.449(3)	C4-C12-C11	119.50(18)

C1-N1-C12	117.96(18)
C10-N2-C11	117.17(18)
N1-C1-C2	123.6(2)
N1-C1-H1A	118.2
C2-C1-H1A	118.2
C3-C2-C1	118.94(19)
C3-C2-H2A	120.5
C1-C2-H2A	120.5
C2-C3-C4	119.5(2)
C2-C3-H3A	120.2
C4-C3-H3A	120.2
C3-C4-C12	117.28(18)
C3-C4-C5	122.57(18)
C12-C4-C5	120.16(17)

Symmetry transformations used to generate equivalent atoms:

#1 -x+1,y,-z+1/2

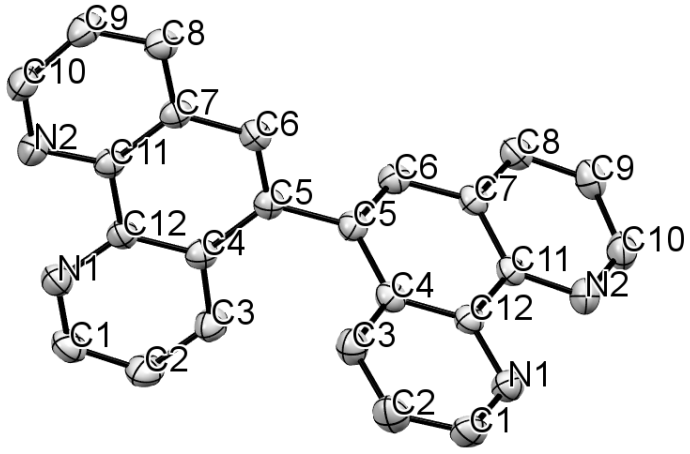

Figure S30. Solid-state molecular structure with the applied numbering scheme of **phenphen** (thermal ellipsoids are at the 50% probability level and hydrogen atoms are omitted for clarity).

Table S6. Crystal data and structure refinement for dp0901_**Ru(phenphen)**.

Identification code	Dp0901
Empirical formula	$C_{62}H_{70}F_{12}N_8O_2P_2Ru$
Moiety formula	$C_{60}H_{62}N_8Ru$, 2(F_6P), 2(CH_4O)
Formula weight	1350.27
Temperature/K	150 K
Wavelength, radiation type	0.71073Å, MoK_α
Diffractometer	KappaCCD
Crystal system	Monoclinic
Space group name	Cc
a	28.7888(14) Å
b	12.25327(9) Å
c	18.8750(18) Å
α	α = 90°
β	β = 114.089(5)°
γ	γ = 90°
Volume	6217.0(8) $Å^3$
Number of reflections	89373
and range used for lattice parameters	6.0° <=θ<= 20.0°
Z	4
Density (calculated)	1.443 Mg/m^3
Absorption coefficient	0.39 mm^{-1}
Absorption correction	Multi-Scan
Max. and min. transmission	0.980 and 0.822
F(000)	2784
Crystal size, colour and form	0.23 x 0.16 x 0.05 mm^3, plate orange
Theta range of data collection	3.1 to 27.1°
Index ranges	-36<=h<=36, -16<=k<=16, -24<=l<=24
Number of reflections:	
collected	89373
independent	13613 [R(int) = 0.072]
observed [I>2sigma(I)]	11804
Completeness to theta = 27.103°	99.3 %
Refinement method	Full-matrix least-squares on F^2
Data / restraints / parameters	89373 / 323 / 897
Goodness-of-fit on F^2	1.02
Final R indexes [I>=2σ (I)]	R_1 = 0.0346, wR_2 = 0.0732
Final R indexes [all data]	R_1 = 0.0473, wR_2 = 0.0781
Largest diff. peak/hole	0.42 and -0.29 e $Å^{-3}$

Table S7. Selected bond lengths [Å] and angles [°] for dp0901_**Ru(phenphen)** with e.s.d.'s given in parentheses.

	Bond distances / Å		Bond angles / °
Ru1 – N1	2.070(4)	N1 – Ru1 – N4	177.17(17)
Ru1 – N4	2.056(4)	N1 – Ru1 – N5	100.96(14)
Ru1 – N5	2.065(3)	N1 – Ru1 – N6	97.06(14)
Ru1 – N6	2.070(3)	N1 – Ru1 – N7	86.24(14)
Ru1 – N7	2.058(3)	N1 – Ru – N10	79.56(14)
Ru1 – N10	2.067(3)	N5 – Ru1 – N7	170.81(13)
C6 – C24	1.499(6)	N6 – Ru1 – N10	173.11(14)
N1 – C2	1.332(6)	C13 – C24 – C6	121.2(4)
N1 – C1	1.372(5)	C23 – C24 – C6	118.2(4)
N2 – C17	1.317(6)	C5 – C6 – C24	119.1(4)
N2 – C18	1.378(6)	C8 – C7 – C12	119.4(4)
N3 – C19	1.352 (6)	N1 – C1 – C10	116.1(4)
N3 – C20	1.337(6)	N2 – C18 – C14	122.8(4)
N10 – C9	1.327(5)	N3 – C19 – C23	122.7(4)
N10 – C10	1.368(5)	N10 – C10 – C12	123.3(4)
C5 – C6	1.360(6)	C14 – C18 – C19	120.3(4)
C13 – C24	1.364(6)	C23 – C19 – C18	118.4(4)
C7 – C12	1.404(6)	C11 – C1 – C10	120.9(4)
C4 – C11	1.408(6)	C12 – C10 – C1	119.9(4)
C14 – C15	1.404(6)	C22 – C23 – C24	122.5(4)
C22 – C23	1.396(6)	C24 – C13 – C14	120.8(4)
C10 – C12	1.415(5)	C6 – C5 – C11	121.6(4)
C1 – C11	1.405(6)	C7 – C12 – C6	124.6(4)
C14 – C18	1.391(6)	C15 – C16 – C17	118.6(4)
C19 – C23	1.426(6)	C5 – C6 – C24 – C13	83.8(6)

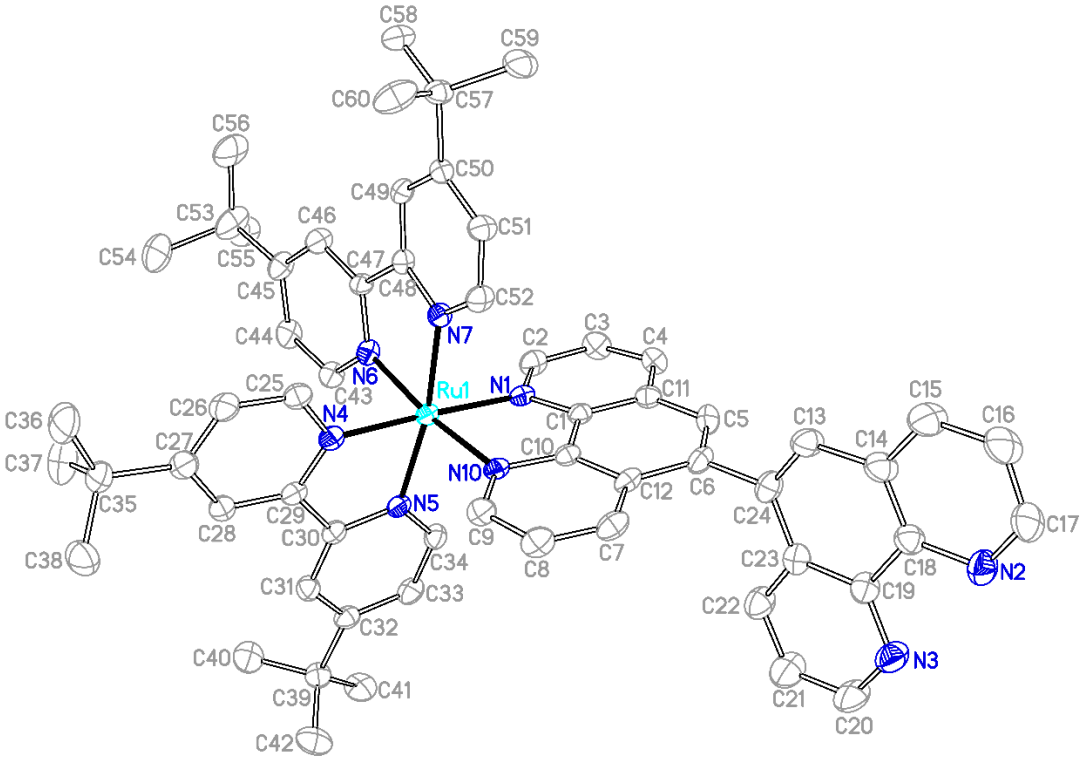

Figure S31. Solid-state molecular structure with the applied numbering scheme of **Ru(phenphen)** in crystals of [Ru(phenphen)]$(PF_6)_2$ • 2 CH_3OH (thermal ellipsoids are at the 50% probability level, hydrogen atoms, disorder and co-crystallized solvent molecules are omitted for clarity).

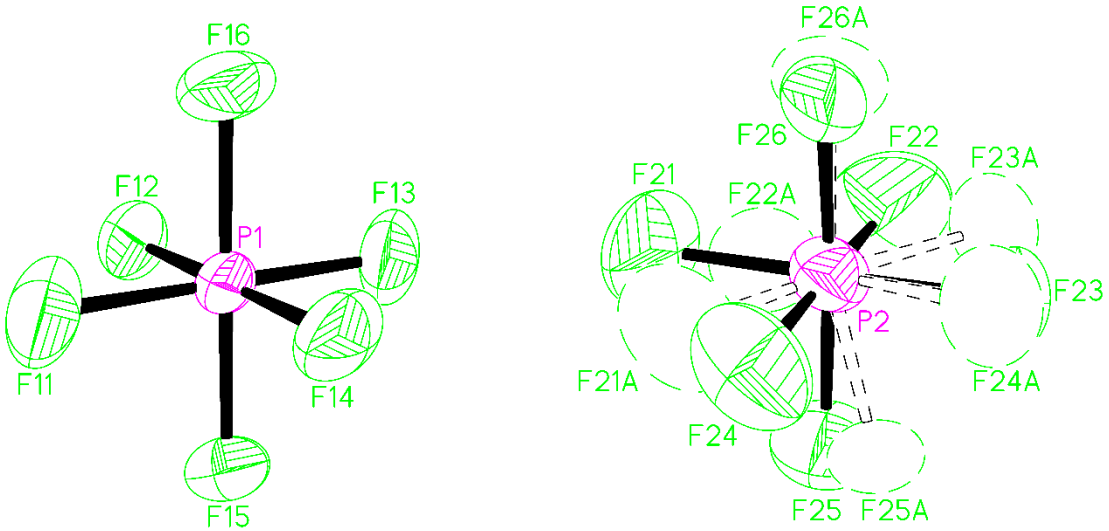

Figure S32. Solid-state molecular structures with the applied numbering scheme of the two PF_6 anions with the observed disorder in one of the anions (right) in crystals of [Ru(phenphen)]$(PF_6)_2$ • 2 CH_3OH (thermal ellipsoids are at the 50% probability level, co-crystallized solvent molecules are omitted for clarity).

7. References

1 A. Stumper, D. Pilz, M. Schaub, H. Görls, D. Sorsche, K. Peuntinger, D. Guldi and S. Rau, 2017, 3799–3810.

2 S. Rau, B. Schäfer, A. Grüßing, S. Schebesta, K. Lamm, J. Vieth, H. Görls, D. Walther, M. Rudolph, U. W. Grummt and E. Birkner, *Inorganica Chim. Acta*, 2004, **357**, 4496–4503.

3 K. Chai, Y. Jiang, T. Han, X. Duan and J. Wang, *Transit. Met. Chem.*, 2018, **43**, 657–664.

4 T. Wu, J. Liu, M. Liu, S. Liu, S. Zhao, R. Tian, D. Wei, Y. Liu, Y. Zhao, H. Xiao and B. Ding, 2019, **100190**, 14224–14228.

5 W. Yang and T. Nakano, *Chem. Commun.*, 2015, **51**, 17269–17272.

6 C. Franco and J.-I. Olmsted, *Talanta*, 1990, **379**, 905–909.

7 A. Graml, T. Neveselý, R. J. Kutta, R. Cibulka and B. König, *Nat. Commun.*, 2020, **11**, 3174.

8 K. Suzuki, A. Kobayashi, S. Kaneko and K. Takehira, 2009, 9850–9860.

9 R. J. Kutta, Universität Regensburg, 2012.

10 R. J. Kutta, T. Langenbacher, U. Kensy and B. Dick, *Appl. Phys. B Lasers Opt.*, 2013, **111**, 203–216.

11 R. J. Kutta, U. Kensy and B. Dick, in *Chemical Photocatalysis*, De Gruyter, 2013, pp. 295–318.

12 T. Hartman, M. Reisnerová, J. Chudoba, E. Svobodová, N. Archipowa, R. J. Kutta and R. Cibulka, *Chempluschem*, 2021, **86**, 373–386.

13 R. J. Kutta, N. Archipowa and N. S. Scrutton, *Phys. Chem. Chem. Phys.*, 2018, **20**, 28767–28776.

14 N. Archipowa, R. J. Kutta, D. J. Heyes and N. S. Scrutton, *Angew. Chemie*, 2018, **130**, 2712–2716.

15 K. Lanzl, M. V. Sanden-Flohe, R. J. Kutta and B. Dick, *Phys. Chem. Chem. Phys.*, 2010, **12**, 6594–6604.

16 COLLECT, *Data Collect. Softw.*, 1998, Nonius B.V., Netherlands.

17 SADABS, *(version 2.06) 2002.*, 2002, Bruker Analytical X-Rau Instruments Inc., Madison,.

18 Z. Otwinowski and W. Minor, *Methods Enzymol.*, 1997, **276**, 307–326.

19 L. Krause, R. Herbst-Irmer, G. M. Sheldrick and D. Stalke, *J. Appl. Cryst.*, 2015, **48**, 3–10.

20 G. M. Sheldrick, *Acta Crystallogr., A*, 1990, **46(6)**, 467–473.

21 G. M. Sheldrick, *Acta Crystallogr., A*, 2008, **64Pt1**, 112–122.

22 G. M. Sheldrick, *Acta Crystallogr., A*, 2015, **71**, 3–8.

23 G. M. Sheldrick, *Acta Cryst.*, 2015, **C71**, 3–8.

24 A. L. Spek, *Acta Cryst.*, 2015, **C71**, 9–18.

25 C. F. Macrae, P. R. Edgington, P. McCabe, E. Pidcock, G. P. Shields, R. Taylor, M.

Towler and J. van de Streek, *J. Appl. Cryst.*, 2006, **39**, 453.

26 S. Kozuch and J. M. L. Martin, *ACS Catal.*, 2012, **2**, 2787–2794.

27 S. Parsons, H. D. Flack and T. Wagner, *Acta Crystallogr., B*, 2013, **69 Pt3**, 249–259.

28 T. D. Pilz, Friedrich-Schiller-Universität Jena, 2011.